Analysis and Topology Optimization of Adaptive Sandwich Plates treated with Magnetorheological Elastomer core layer

Maryam Zare

A Thesis

In

The Department

Of

Mechanical, Industrial and Aerospace Engineering

Presented in Partial Fulfillment of the Requirements for The Degree of

Master of Mechanical Engineering

Concordia University

Montreal, Quebec, Canada

October 2023

CONCORDIA UNIVERSITY
School of Graduate Studies

This is to certify that the thesis prepared

By: Maryam Zare

Entitled: **Analysis and Topology Optimization of Adaptive Sandwich Plates treated with Magnetorheological Elastomer core layer**

and submitted in partial fulfillment of the requirements for the degree of

Master of Mechanical Engineering

complies with the regulations of the University and meets the accepted standards with respect to originality and quality.

Signed by the final examining committee:

_____ Chair
Dr. Hang Xu

_____ Examiner
Dr. Lan Lin

_____ Examiner
Dr. Hang Xu

_____ Thesis Supervisor
Dr. Ramin Sedaghati

Approved by _____
Dr. Sivakumar Narayanswamy, Graduate Program Director

_____
Dr. Mourad Debbabi, Dean

Gina Cody School of Engineering and Computer Science

Date October 2023

ABSTRACT

Analysis and Topology Optimization of Adaptive Sandwich Plates treated with Magnetorheological Elastomer core layer

By Maryam Zare

Structural vibration control is a promising method for mitigating the detrimental effects of excessive vibration in structures. It involves monitoring the dynamic behavior of a structure and implementing control strategies to reduce the vibration levels of the structure. Among various control methodologies, the semi-active control method adeptly combines the reliability characteristic of passive systems with the adaptability inherent in fully active systems, without requiring complex control hardware. Smart materials play a crucial role in implementing semi-active vibration control, and among them, magnetorheological (MR) materials have garnered substantial attention for their remarkable properties, including rapid response times and low energy consumption. Compared with MR fluids (MRFs) which can only provide variable damping, Magnetorheological elastomers (MREs) have field dependent viscoelastic properties in which both stiffness and damping properties can be effectively altered using the applied magnetic field. By incorporating MREs into the core of sandwich plates, it becomes possible to modify the continuous plate's vibration characteristics on-demand through application of an external magnetic field. Although employing complete coverage of the MRE core layer within a sandwich plate is likely to yield the best results in reducing vibration levels, it is essential to consider practical factors like mass limitations. Therefore, optimizing the topology of the MRE layer with a constrained volume fraction is of practical importance. The goal of the topology optimization process is to attain the desired vibration control performance while concurrently minimizing the mass or volume of the MRE layer. This enables the efficient utilization of MRE-based vibration control systems in real-world applications, where optimizing resources is crucial.

To achieve this end, first a finite element model has been formulated to evaluate the vibration behavior of MRE-based sandwich plate under dynamic loading. The plate is discretized with rectangular elements, each having 28 degrees of freedom and 4 nodes, enabling accurate estimation of the MRE-based sandwich plate's vibration characteristics.

An optimization problem based on the method of moving asymptotes (MMA), is subsequently formulated to identify the optimal topology of the MRE layer within the sandwich plate to minimize dynamic compliance yielding reduction in vibration amplitude. For material properties interpolation, an MRE-based penalization (MREP) model, based on solid isotropic material with penalization (SIMP) method, has been developed. To validate the accuracy of the proposed methodology, several numerical examples considering MRE-based sandwich plates under different loading and boundary conditions are provided. These examples illustrate the effectiveness of the proposed design optimization methodology for topology optimization of MRE-based sandwich panels to mitigate the vibration.

,

Acknowledgments

Firstly, I would like to express my sincere gratitude and appreciation to my supervisor, Professor Ramin Sedaghati, for giving me the opportunity to join his research team, and for his patience, support, supervision, and exceptional guidance throughout my research. Also, financial support from the Natural Sciences and Engineering Research Council of Canada is gratefully acknowledged.

I sincerely acknowledge my mother, father, and younger sister for endlessly supporting me whenever I encountered challenges in my life. They have always been my solid support along my academic and professional life journey with their continuous encouragement and inspiration.

I greatly thank all my dearest officemates, Afroz Hajimoradi, Seyed Alireza Moezi, Amin Saber, Sina Tavassoli Naini, Shakila Zabiholla, Hooman Zoka, Mostafa Abdalaziz, Mohamed Ghanem, Hamid Nourani, Hossein Mohammad Taheri and Ilda Abdollahi who have helped me with their constant companionship, inspiration, and support in these years.

Table of Contents

List of Tables

List of Figures

Nomenclature

TOP	Topology opotimisation method
$SIMP$	Solid isotropic material with penalization
MREP	Magnetorheological elastomer material with penalization
SLP	Sequential Linear Programming
MMA	Method of moving asymptotes
GMMA	Generalized method of moving asymptotes
PEMAP-P	Piezoelectric material with penalization and polarization
C	Dynamic compliance
V_0	Volume fraction
p	Penalization factor
B	Magnetic flux density
G	Shear modulus
G'	Storage modulus
G''	Loss modulus
N_c	Number of coils
G'	Storage modulus

G''	Loss modulus
G^*	Density
x_e	Elemental relative density
FEM	Finite element method
w	Deflection
u	x-axis displacement
v	y-axis displacement
φ	Rotation angle
β	Shearing deformation
ω	Natural frequency
ε	Normal strain
γ	Shear strain
T	kinetic energy
U	Potential energy
M	Mass matrix
K	Stiffness matrix
F	Force vector
v	Poisson's ratio

h_c	Constraining layer thickness
h_b	Basic layer thickness
h_m	MRE layer thickness

Chapter 1: Introduction, dissertation objectives

1.1 Introduction

As vibration often poses a safety concern and makes discomfort, the suppression of structural vibration is one of the major research subjects in engineering. It is well known that structural vibration control is one of the most promising methods for mitigating a variety of detrimental effects of excessive vibration in structures. In this approach, the main goal is to monitor the dynamic behavior of a structure utilizing passive, active and semi-active control strategies to mitigate the unreasonable vibration. Passive control systems require no external power source and include passive viscoelastic materials, supplementary dampers such as tuned mass damper (TMD) and tuned liquid column damper (TLCD), and base isolation systems. The merits of this approach include the typically straightforward nature of the devices and the assurance of system stability. However, passive treatments are only effective within a restricted range of external excitations [1,2]. Active vibration control is the active application of force using actuators in an equal and opposite manner to the forces imposed by external vibration. Using this approach, a significant vibration reduction over a broad range of frequency may be achieved. When high performance is required, active control can be used; this involves a set of sensors (strain, acceleration, velocity, force, ...), a set of actuators (force, inertial, strain,...), and a closed-loop control algorithm (feedback or feedforward) [3]. Compared with the passive vibration control strategy, the semi-passive techniques offer higher robustness and performance gain. Compared with active damping systems, their implementation does not require any sophisticated signal processing systems or any complex control hardware [4]. Semi-active control strategies have the fail-safe and reliability features of passive systems while miniating the adaptability of the fully active systems without requiring complex control hardware and large power. Smart materials are widely used in implementing semi-active vibration control in structures. These types of materials have properties that respond to changes in their environment. This means that one of their properties can be altered by an external condition, such as temperature, light, pressure, electricity and magnetic field. These materials can change their dimensions, solubility, color, shape and stiffness, etc., upon a specific point. Smart materials can be designed with various responses and actuation mechanisms based on the requirements of applications [5]. A variety of smart materials including alloys, composites, gels, and polymers have been applied for different applications from the aerospace industry to

medical technologies. These include: piezoelectric [6], biomimetic [7], thermochromic [8], electrorheological [9], thermoelectric [10], photochromic [11], magneto-sensitive [12], magneto-active [13], shape memory alloys [14] and magnetorheological (MR) materials [15].

Among smart materials, MR fluids and MR elastomers have been effectively utilised in semi-active vibration control applications. The viscoelastic and rheological properties of MR materials can be changed instantly through the application of an external magnetic field. MR elastomers are the solid-state analogue of MR fluids in which micron-sized magnetic particles (typically iron particles) are embedded in an elastomeric matrix.

MRE can be effectively used as the core layer in sandwich structures to develop an innovative adaptive continuous structure with field-dependent damping and stiffness without any leakage issues as often encountered in MR fluid-based sandwich panels. While sandwich structures fully treated with MREs may provide superior performance compared with those partially treated with MREs, it is of high importance to find optimal topology distribution of MREs due to practical considerations.

In this dissertation, the optimum topology distribution of the MRE layer in a sandwich plate is investigated. The adaptive sandwich plate consists of an MR elastomer layer embedded between two thin elastic plates. The dynamic and vibration response of the structure is evaluated using the developed finite element method in MATLAB environment. Rectangular elements with 4 nodes, each with 7 degrees of freedom (for a total of 28 DOFs), are employed to model the sandwich plate. To obtain the optimum partial treatment of the MR layer for the best performance in vibration control in wide-band frequency range, dynamic compliance is defined as the objective function to be minimized. The density of each element is defined as the variables in the optimization problem. In this study, the solid isotropic material with penalization (SIMP) method, is extended for material properties interpolation which leads to the development of MRE-based penalization (MREP) model. Method of moving asymptotes (MMA) which is based on a special type of convex approximation [19] has been utilized to solve the optimization problem. In the following, a literature review has been conducted. Then, the motivations and objectives are discussed. Finally, the current organization of the thesis is described.

1.2 **Magnetorheological Elastomers**

Magnetorheological materials are classified as a functional smart material possessing tunable rheological and viscoelastic properties such as yield stress, shear stress, dynamic moduli, and damping property when an external magnetic field is applied [16-20]. According to their host medium, MR materials generally include several different types such as MR fluids (MRFs), MR foams, MR gels, and MR elastomer s(MREs) [15]. MREs consist of three basic components: micron-sized magnetic particles, nonmagnetic elastomeric matrices, and additives [21]. For the magnetic particles, the micron-sized carbonyl iron powder invented by BASF in 1925 is widely used [22] due to its high magnetic saturation limit. For the elastomeric matrix, there are several potential candidates such as natural rubber [23], silicone rubber [24] and polydimethylsiloxane (PDMS) [25], that can be effectively used. In the presence of an external magnetic field, MREs exhibit field-dependent damping and stiffness properties. The application of a magnetic field alters the loss and storage moduli of MREs. This unique feature enables the effective utilization of MREs in the development of high-bandwidth adaptive vibration absorbers.

According to the fabrication process, MREs can be classified into two different groups namely, isotropic and anisotropic MREs as shown in Figure 1-1. For the fabrication, the magnetic particles and the liquid elastomeric matrix, along with some additives, are first thoroughly mixed and degassed. Subsequently, the mixture undergoes vulcanization, which can occur either at room temperature, referred to as room-temperature vulcanizing (RTV [26]), or at a high temperature exceeding 120°C, known as high-temperature vulcanizing (HTV [27]). If the vulcanization process takes place in the presence of a magnetic field, the magnetic particles have the ability to move within the matrix and gradually form chain-like structures aligned with the direction of the field, resulting in the creation of anisotropic MRE. Curing in the absence of a magnetic field, results in uniform random dispersions of the magnetic particles in the matrix after vulcanization forming an isotropic MRE.

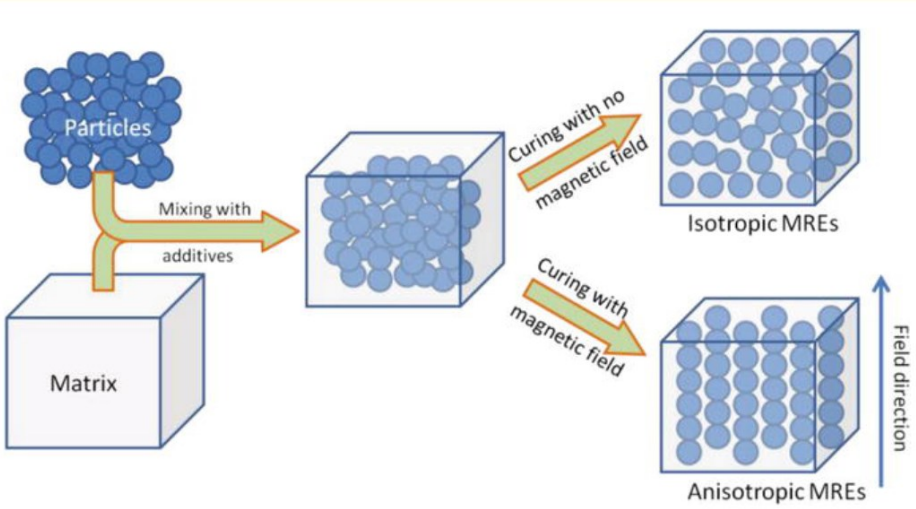

Figure 1-1: A schematic fabrication process of an isotropic and anisotropic MRE sample [21]

1.3 **MRE-based Sandwich Plate**

Sandwich plates, which consist of two stiff thin face sheets separated by a flexible core, are commonly used in many engineering applications for vibration damping in aerospace, automotive, and civil engineering. The conventional passive sandwich plates are generally designed to mitigate vibration within a limited and specific frequency range. By incorporating MREs as the core material in sandwich plates, the mechanical properties of the sandwich structure can be adaptively controlled in response to a magnetic field. This allows for the mitigation of vibrations across a broad range of frequencies, even under unpredictable environmental conditions.

There are some studies on the dynamic characteristics of MRE-based sandwich structures, wherein an array of various modeling techniques and experimental approaches have been developed and reported. Nayak et al. [28] evaluated the forced vibration of an MRE-cored sandwich beam. In their study, a magnetorheological elastomer (MRE) was fabricated with carbonyl iron particles mixed with silicon rubber as the matrix. The sandwiched beam consisted of an MRE core layer sandwiched between elastic layers. They also conducted experimental tests to investigate the effect of a magnetic field on the vibration response of the sandwich beam. A schematic view of their experimental setup is illustrated in Figure 1-2.

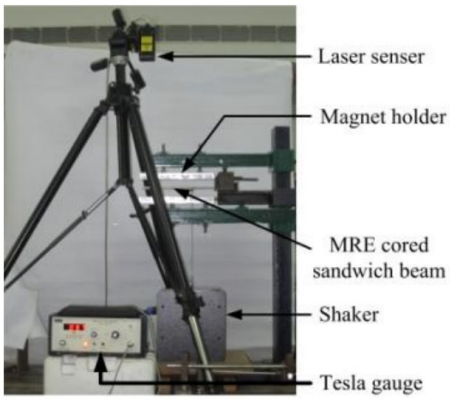

Figure 1-2: The experimental setup for the vibration analysis of the MRE-based sandwich beam [28]

Babu et al. [29] conducted an investigation into the dynamic performance of an MRE-embedded tapered laminated composite sandwich plate. In their model, the MRE serves as the core, while the tapered composite plates are utilized as the face plates. They developed numerical codes using the Finite Element Method (FEM) and validated the accuracy of their numerical approach through experimental tests. Choi et al. [30] examined the dynamic characteristics of an MRE core-embedded smart sandwich beam. They improved an analytical model based on Frostig's high-order beam theory to incorporate viscoelastic material properties and their frequency dependence. In their simulation, they explored different boundary conditions and variations in the portions of the MRE core.

The stochastic micro-vibration response of a clamped–free sandwich beam with an MR elastomer core was explored by Ying et.al [31]. They derived the partial differential equation of motion for the sandwich beam by considering dynamic equilibrium, constitutive relations, and geometric factors. Additionally, they developed a frequency-domain solution method for analyzing the stochastic micro-vibration response, utilizing concepts of frequency-response functions, power spectral density functions, and spatial eigensolution.

In recent studies, more complex sandwich plates incorporating MRE layers have been investigated. In a study conducted by Li et al. [32], the static and dynamic performance of MRE sandwich plates (MRESPs) was examined, wherein the MRE core comprises two copper wire layers, two inner metal layers, and one MRE layer. A schematic view of the structure is presented in Figure 1-2

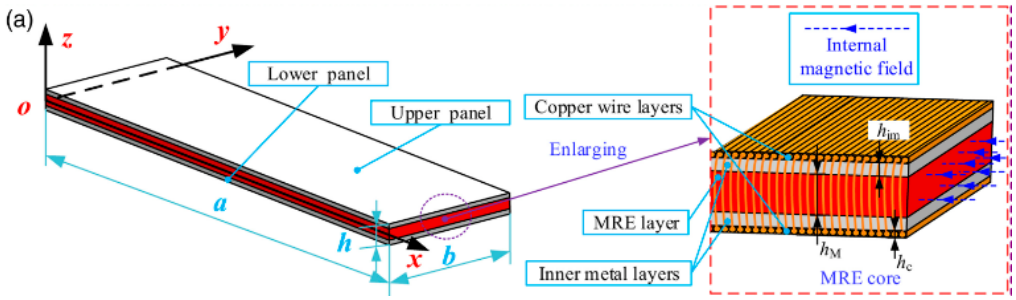

Figure 1-3: Schematic diagram of an MRESP [32]

1.4 Topology Optimization of MRE layer in Sandwich Plates

The placement of MRE layers in composite sandwich structures can significantly affect the overall mechanical properties of the structure (the stiffness and damping), and thus it's vibration control characteristics. Therefore, it is essential to study the optimal location of the MRE layer to improve the performance of the sandwich plate. By strategically positioning the MREs, it is possible to optimize the vibration damping or stiffness characteristics of the composite plate while reducing the weight of the structure.

In a study conducted by Vemuluri et.al [33], the optimal locations of magnetorheological elastomer (MRE) segments within partially treated tapered composite MRE sandwich plates are investigated. Their study formulates an optimization problem with the aim of maximizing natural frequencies and loss factors, employing the finite element method in conjunction with a Genetic Algorithm (GA). Snamina [34] conducted a study involving a rectangular sandwich plate with an MR fluid material as the core layer. In their research, they define an optimization problem with the objective of identifying the optimal placement of active segments within the MRF layer based on calculations of energy dissipated by this layer.

Previous studies have primarily focused on determining the optimal locations of discrete MRE layers, without addressing the optimal topology distribution of MREs. Topology optimization (TO) is a design optimization method used to find the best distribution of material within a predefined domain, given a set of loads, constraints, and boundary conditions, in order to achieve optimal structural performance. While initially developed for mechanical design problems, this concept has expanded to various other physical disciplines, such as fluids, acoustics, electromagnetics, optics, and their combinations [35]. The methodology combines the finite

element method with optimization techniques to either maximize or minimize an objective function [36]. Consequently, the predefined domain is discretized into a finite number of elements, and the design variables for the optimization problem are the properties assigned to these elements. Depending on the continuity of the main domain, topology optimization is classified into two types: discrete and continuous TO. In discrete TO, the objective is to determine the optimum number, positions and connectivity of structural members. Topology optimization methods for continuous structures fall into several categories, including homogenization-based method, density-based methods, evolutionary methods and boundary variation methods. Among these approaches, density-based methods are the most widely used and are commonly employed in commercial TO software [37]. This method primarily relies on the finite element method for analysis, with the variable often defined as the element's material density. Additionally, the material properties of each element are interpolated as a function of density design variables. The choice of an appropriate interpolation function holds high significance in this method, and several interpolation functions have been proposed, such as the SIMP method [38] and rational approximation of material properties (RAMP) method [39], to obtain a solid/void form.

In some studies, topology optimization problem has been formulated to maximize vibration suppression by identifying the best distribution of damping layers. In a research conducted by Kang [41], reducing the residual vibration of shell structures under impact loads was investigated by optimizing the distribution of the damping layer. In their optimization problem, an integrated square performance measure of residual vibration was used as the objective function, and an efficient adjoint method was used to calculate the sensitivities. The topology optimization was implemented based on the common SIMP method.

Kim et. al [42], obtained the optimum distribution of damping layers in a shell structure for mitigating the vibration by maximization of the damping effect (the modal loss factor). Some researches focus on achieving the optimum distribution of piezoelectric actuators in structures to optimize their performance. Guzmán et.al [43] determined the optimal layout of piezoelectric transducers. In their approach, they aimed to maximize two objective functions: the trace of the controllability gramian matrix and the trace of the observability gramian matrix. They based their optimization on a SIMP material interpolation model, a spatial filter, and the Sequential Linear Programming (SLP) method with moving limits.

Abbas et.al [44] provided a Matlab code for topology optimization of piezoelectric actuators based on MMA method. In their study, the extension of SIMP approach known as PEMAP-P (piezoelectric material with penalization and polarization) was used for the material interpolation.

Noh et.al [45] developed an optimization procedure to obtain the optimal layouts for piezoelectric energy harvesting devices (EHDs) considering the effect of static and harmonic dynamic mechanical loads. In their model, material properties including the anisotropic linear elasticity coefficients, piezoelectric coefficients, and permittivity coefficients were interpolated using the SIMP approach.

1.5 **Motivation and Objectives**

In the present study, the overall goal is to develop a design optimization methodology for identifying the optimal distribution of the MRE layer in a sandwich plate to achieve maximum reduction in vibration levels. The core of the structure comprises an MRE layer sandwiched between two elastic thin plates. A finite element model has been developed using 4-node rectangular elements with 28 degrees of freedom to analyze the adaptive MRE-based sandwich plate structure. Dynamic compliance is defined as the objective function to be minimized, and the design variables are defined as the density of each element. In this study, the SIMP method is extended for material properties interpolation, resulting in the development of the MRE-based penalization (MREP) method. The optimization problem formulated is solved using the MMA method, which is based on a special type of convex approximation [46]. Addressing the research gap, the specific objectives of the present research study are as follows:

i. Development of a finite element model to accurately extract the dynamic response behavior of MRE-based sandwich plates under different boundary conditions.

ii. Formulating a multidisciplinary design topology optimization problem to identify the optimum layout of the MRE layer to minimize the dynamic compliance of the sandwich plate subject to weight constraint.

iii. Investigating the effect of loading parameters on the optimum layouts of MRE layer

iv. Considering the effect of volume fraction on the optimum distribution of the MRE layer

v. Studying the impact of optimized MRE layouts on vibration mitigation under different excitations.

1.6 **Organization of the Dissertation**

The dissertation includes five chapters describing the research findings and results in a systematic order. Chapter 1 presents an introduction to the research dissertation incorporating pertinent literature review, an introduction to magnetorheological elastomers, MRE-based sandwich plates, topology optimization of MRE layer in sandwich plates, motivations and objectives, and organization of the dissertation.

In chapter 2, a finite element has been developed to analyze the dynamic performance of a MRE-based sandwich plate under various combinations of applied magnetic fields, loadings, and boundary conditions. In order to achieve the optimum layout of MRE layer, a topology optimization method is proposed in chapter 3. Chapter 4 provides the optimum topologies of MRE layer considering different loading conditions. The effect of optimum topologies on reducing the vibration level of the structure has been investigated in this chapter. Chapter 5 discusses and summarizes the major findings and contributions, as well as some future remarks.

Chapter 2: Finite Element Modeling of MRE-based Sandwich Plates

2.1 Introduction

Finite Element (FE) method is a powerful numerical tool widely used in engineering and science to analyze and design complex structures and systems. The FE is based on the concept of dividing the structure or system into a finite number of small and simpler elements, which are then connected to each other to form the complete system.

FE method has been utilized in this study to analyze dynamic response of MRE-based sandwich plates under varied magnetic field, loading conditions as well as different boundary conditions. The sandwich plates consist of a MRE core layer integrated between two elastic upper and lower thin plates. To develop an accurate FE model, it is essential to select appropriate element types and sizes, define the material properties and boundary conditions, and apply the correct loading conditions. The accuracy of the model can be verified by comparing the simulation results with experimental data or available analytical solutions.

In this chapter, the FE is used to investigate the response of a sandwich plate with a magneto-rheological elastomer (MRE) core layer under different magnetic and mechanical loading and boundary conditions. The structure is discretized into a number of small, interconnected rectangular elements. Each element is characterized by its stiffness and mass matrix, which are calculated based on the mechanical energy of the element. Kirchhoff plate theory is used to model the kinematics of the sandwich plate. Once the stiffness and mass matrixes of each individual element are obtained, they are assembled to form the global stiffness and mass matrices of the entire structure. This involves arranging the individual element stiffness and mass matrices in a particular way that accounts for their interconnectivity, ensuring that all degrees of freedom are accounted for.

Subsequently, the governing equations of motion be derived in the FE format for the entire structure. The equations of motion describe how the structure responds to external loads, offering a powerful tool for predicting its response behavior under different loading conditions.

2.2 Development of FE Model for a MRE-based Sandwich Plate

In this section FE model of the sandwich structure is developed. The schematic view of the sandwich plate is shown in Figure 2-1.

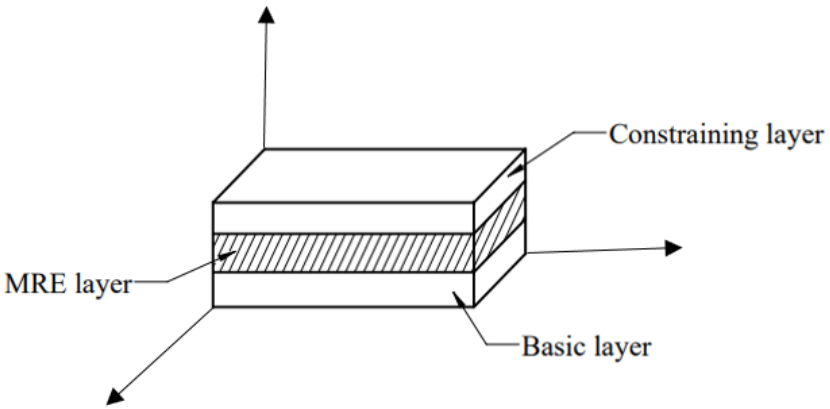

Figure 2-1: Schematic view of the MRE core sandwich plate

As depicted, the structure comprises two elastic layers at the top and bottom, serving as constraining and base layers, respectively, with an isotropic MRE layer integrated as the core. The FE model for the sandwich plate is established based on the subsequent assumptions:

1. Kirchhoff plate theory is used for modeling the top and bottom layers. Thus, transverse shear strains and deformation through the thickness are ignored. It is assumed that there are no stretching and shear deformation in mid-plane of elastic layer except bending deformation.
2. The moment of the inertia of each layer is ignored.
3. The layers are considered completely bonded to each other without any slippage.
4. The MRE core operates under small shear deformation thus linear viscoelastic behavior is assumed.

2.2.1 Kinematics of Sandwich Plates

In Figure 3-1, the geometric deformation relationship among distinct layers of a typical sandwich plate is illustrated. The deflected and undeflected cross-sections are presented on the right and left sides, respectively. Dotted lines indicate the mid-plane of each layer.

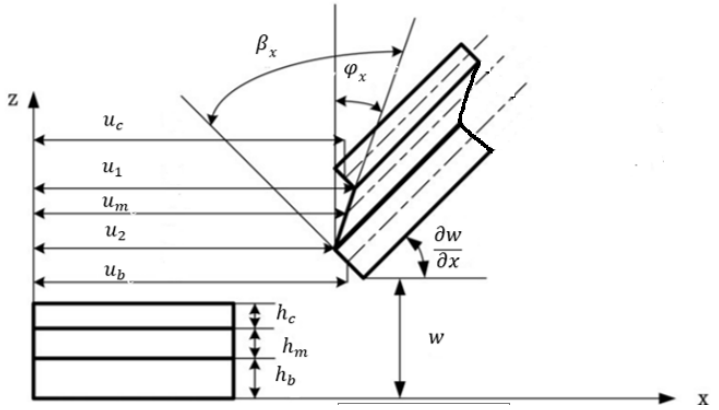

Figure 2-2: The deformation schematic view of the MRE core sandwich plate [48]

u_c, u_m and u_b represent the mid-plane displacements along x direction corresponding to the constraining layer, MRE layer, and the bottom layer, respectively. Also, u_1 and u_2 are the displacements of the top and bottom surface of the MRE layer along the x direction; $\frac{\partial w}{\partial x}$, φ_x, and β_x are the rotation angle of the sandwich plate, the rotation angle of MRE layer and the shearing deformation of the MRE layer all around y-axis, respectively. The thicknesses of the constraining layer, MRE layer, and the bottom layer are denoted as h_c, h_m, and h_b, respectively.

Based on Kirchhoff's first-order shear deformation theory (FSDT), the displacement of any point within the plate can be formulated as [49-50]:

$$\begin{aligned} u(x,y,z) &= u_0(x,y) - z\left(\frac{\partial w}{\partial x}\right) \\ v(x,y,z) &= v_0(x,y) - z(\frac{\partial w}{\partial y}) \\ w(x,y,z) &= w(x,y) \end{aligned} \tag{2.1}$$

where, u and v are the displacements along the x and y axes, respectively; w is the deflection through the thickness of the plate; u_0 and v_0 are the midplane displacements along the x and y axes, respectively. Additionally, the notation z is used to represent the distance of any point from the midplane.

Considering $z = \frac{-h_c}{2}$ and $u_0 = u_c$ for the bottom surface of the constraining layer, and $z = \frac{h_b}{2}$ and $u_0 = u_p$ for the top surface of the bottom layer, and using the first relation in Eq. (2.1), the displacements of the top and bottom surfaces of the MRE layer along the x-axis are determined as:

$$u_1 = u_c + \frac{h_c}{2}\frac{\partial w}{\partial x}$$
$$u_2 = u_p - \frac{h_b}{2}\frac{\partial w}{\partial x} \tag{2.2}$$

Similarly, applying the second relation in Eq. (2.1), leads to the following expression for the *y*-direction displacements of the top and bottom surfaces of the MRE layer as:

$$v_1 = v_c + \frac{h_c}{2}\frac{\partial w}{\partial y}$$
$$v_2 = v_p - \frac{h_b}{2}\frac{\partial w}{\partial y} \tag{2.3}$$

Taking into account the assumption that there is no stretching in the MRE mid-plane, the mid-plane displacement of the MRE layer along the *x* direction can be derived as:

$$u_m = \frac{u_1 + u_2}{2} \tag{2.4}$$

By substituting the values of u_1 and u_2 from Eq. (2.2) into Eq. (2.4), the following expression for the *x*-direction displacement of the MRE layer can be derived:

$$u_m = \frac{1}{2}\left[(u_c + u_b) + (\frac{h_c - h_b}{2})\frac{\partial w}{\partial x}\right] \tag{2.5}$$

Applying the same procedure, the mid-plane displacement of the MRE layer in the *y*-direction is determined as:

$$v_m = \frac{1}{2}\left[(v_c + v_b) + (\frac{h_c - h_b}{2})\frac{\partial w}{\partial y}\right] \tag{2.6}$$

Considering Figure 2-2, and the relation in Eq. (2.2), the rotation angle of the MRE layer, φ_x, and the shearing deformation of this layer along *y* axis, β_x, can be formulated as:

$$\varphi_x = \frac{1}{h_m}\left[(u_c - u_b) + (\frac{h_c + h_b}{2})\frac{\partial w}{\partial x}\right]$$
$$\beta_x = \frac{1}{h_m}\left[(u_c - u_b) + (\frac{h_c + h_b}{2} + h_v)\frac{\partial w}{\partial x}\right] \tag{2.7}$$

Likewise, the shear deformation of the MRE layer around the *x*-axis can be determined as:

$$\beta_y = \frac{1}{h_m}\left[(v_c - v_b) + (\frac{h_c + h_b}{2} + h_v)\frac{\partial w}{\partial y}\right] \tag{2.8}$$

According to the thin plate bending theory, the induced normal strains, ε_{Tx}, ε_{Ty}, as well as the shear strain, γ_{Txy}, pertaining to each layer corresponding to tensile load can be expressed as:

$$\varepsilon_{Tx} = \frac{\partial u}{\partial x} \quad \varepsilon_{Ty} = \frac{\partial v}{\partial y} \quad \gamma_{Txy} = \frac{\partial u}{\partial y} + \frac{\partial v}{\partial x} \tag{2.9}$$

Moreover, the corresponding tensile and shear stress within each layer characterized by the elastic modulus E and Poisson's ratio v, is defined as:

$$\sigma_T = \frac{E}{1-v^2}\begin{bmatrix} 1 & v & 0 \\ v & 1 & 0 \\ 0 & 0 & \frac{1-v}{2} \end{bmatrix}\{\varepsilon_{Tx} \ \varepsilon_{Ty} \ \gamma_{Txy}\}^T \tag{2.10}$$

The strain within each layer resulting due to bending is formulated as:

$$\varepsilon_{bx} = \frac{\partial^2 w}{\partial x^2} \quad \varepsilon_{by} = \frac{\partial^2 w}{\partial x y^2} \quad \gamma_{bxy} = 2\frac{\partial^2 w}{\partial x \partial y} \tag{2.11}$$

Likewise, the relevant stress within each layer is designated as:

$$\sigma_b = \frac{Eh^3}{12(1-v^2)}\begin{bmatrix} 1 & v & 0 \\ v & 1 & 0 \\ 0 & 0 & \frac{1-v}{2} \end{bmatrix}\{\varepsilon_{bx} \ \varepsilon_{by} \ \gamma_{bxy}\}^T \tag{2.12}$$

It's worth mentioning, h is the thickness of the corresponding layer.

2.2.2Finite Element Model

A three-layer sandwich rectangle element containing four nodes has been formulated to develop FE model of the MRE-based sandwich plate. Each node possesses seven DOFs, including the displacement of the constraining and basic layers along the x and y directions, denoted as u_c, v_c, u_b, v_b, respectively, as well as the plate's transverse deflection, w. Additionally, there are rotations about the x and y axes, represented as θ_x, θ_y, respectively. Figure 2-3 depicts a schematic diagram of the element, illustrating only the seven degrees of freedom of the first node for clarity.

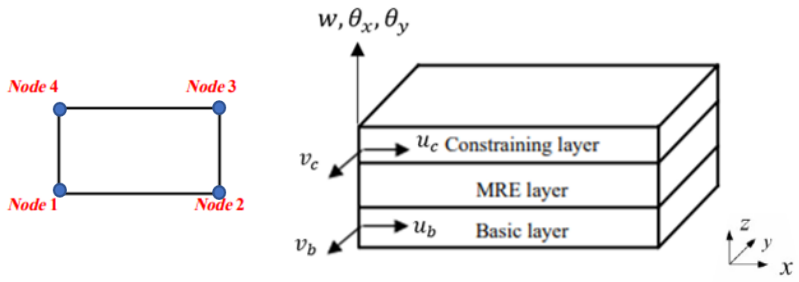

Figure 2-3: The schematic diagram of the 4-noded element

The element displacement function can be expressed in matrix form as:

$$W(t) = \{u_c, v_c, u_b, v_b, w, \theta_x, \theta_y\} \tag{2.13}$$

Also, the nodal displacement vector is given as:

$$W^e(t) = \{u_{ci}, v_{ci}, u_{pi}, v_{pi}, w_i, \theta_{xi}, \theta_{yi}\} \quad i = 1,2,3,4 \tag{2.14}$$

The element displacement vector can be expressed in terms of the nodal displacement vector as:

$$W = NW^e \tag{2.15}$$

where the 7×28 matrix of N is the shape function matrix of the element. One essential aspect of the elements is the definition of shape functions, which are mathematical functions used to described the displacement within the element using element nodal DOFs. To derive the shape function of the developed element, the interpolation polynomial matrix of P is applied to express the element displacement matrix as:

$$W = Pa \tag{2.16}$$

where

$$P = \begin{bmatrix} 1 & x & y & xy & 0 & 0 & 0 & 0 & 0 & 0 & 0 & 0 & 0 & 0 & 0 & 0 & 0 & 0 & 0 \\ 0 & 0 & 0 & 0 & 1 & x & y & xy & 0 & 0 & 0 & 0 & 0 & 0 & 0 & 0 & 0 & 0 & 0 \\ 0 & 0 & 0 & 0 & 0 & 0 & 0 & 0 & 1 & x & y & xy & 0 & 0 & 0 & 0 & 0 & 0 & 0 \\ 0 & 0 & 0 & 0 & 0 & 0 & 0 & 0 & 0 & 0 & 0 & 0 & 1 & x & y & xy & 0 & 0 & 0 \\ 0 & 0 & 0 & 0 & 0 & 0 & 0 & 0 & 0 & 0 & 0 & 0 & 0 & 0 & 0 & 0 & 1 & x & y \\ 0 & 0 & 0 & 0 & 0 & 0 & 0 & 0 & 0 & 0 & 0 & 0 & 0 & 0 & 0 & 0 & 0 & 0 & 1 \\ 0 & 0 & 0 & 0 & 0 & 0 & 0 & 0 & 0 & 0 & 0 & 0 & 0 & 0 & 0 & 0 & 0 & -1 & 0 \end{bmatrix} \tag{2.17}$$

$$\begin{bmatrix} 0 & 0 & 0 & 0 & 0 & 0 & 0 & 0 & 0 \\ 0 & 0 & 0 & 0 & 0 & 0 & 0 & 0 & 0 \\ 0 & 0 & 0 & 0 & 0 & 0 & 0 & 0 & 0 \\ 0 & 0 & 0 & 0 & 0 & 0 & 0 & 0 & 0 \\ x^2 & xy & y^2 & x^3 & x^2y & xy^2 & y^3 & x^3y & xy^3 \\ 0 & x & 2y & 0 & x^2 & 2xy & 3y^2 & x^3 & 3xy^2 \\ -2x & -y & 0 & -3x^2 & -2xy & -y^2 & 0 & -3x^2y & -y^3 \end{bmatrix}$$

and $a = [a_1\ a_2\ a_3\ \dots\dots a_{28}]^T$ is the coefficient matrix, which is determined through the application of the element nodal conditions.

The element comprises four nodes, and the coordinates (x, y) for each node are known. Applying Eq. (2.14) to Eq. (2.16) and inserting the nodal coordinate values associated with each node into the expression for P, the coefficient matrix a can be expressed as:

$$a = CW^e \tag{2.18}$$

Here, C is a 28×28 matrix that depends on the known node coordinates. By substituting Eq. (2.18) into Eq. (2.16) and comparing with Eq. (2.15), the shape function matrix can be expressed as:

$$N = [N_1\ N_2\ N_3\ N_4\ N_5\ N_6\ N_7\ ] = PC \tag{2.19}$$

Substituting Eq. (2.19) into Eq. (2.15), the seven displacement components of the plate element can be expressed using the shape functions as:

$$\begin{array}{llll} u_c = N_1W^e, & v_c = N_2W^e, & u_b = N_3W^e, & v_b = N_4W^e \\ w = N_5W^e, & \theta_x = N_6W^e, & \theta_y = N_7W^e & \end{array} \tag{2.20}$$

By substituting Eq. (2.20) into Eq. (2.5) through Eq. (2.8), the MRE layer displacements and its shearing deformations can be expressed as:

$$u_m = N_8W^e, \quad v_m = N_9W^e, \quad \beta_x = N_{10}W^e, \quad \beta_y = N_{11}W^e \tag{2.21}$$

The shape functions of the MRE layer can be determined from:

$$\begin{aligned} N_8 &= \frac{1}{2}\left[(N_1 + N_3) + \left(\frac{h_c - h_b}{2}\right)(-N_7)\right] \\ N_9 &= \frac{1}{2}\left[(N_1 + N_4) + \left(\frac{h_c - h_b}{2}\right)(N_6)\right] \end{aligned} \tag{2.22}$$

$$N_{10} = \frac{1}{h_m}\left[(N_1 - N_3) + \left(\frac{h_c + h_b}{2} + h_m\right)(-N_7)\right]$$
$$N_{11} = \frac{1}{h_m}\left[(N_2 - N_4) + (\frac{h_c + h_b}{2} + h_m)(N_6)\right]$$

2.3 Equations of Motion

To derive the equations of motion for the element, the Hamilton's principle [47] is employed, which can be mathematically described as:

$$\delta \int_{t1}^{t2} (T - V)dt = 0 \tag{2.23}$$

Here, T and V represent the kinetic and potential energy of the sandwich plate, respectively, and they are determined as follows.

The kinetic energy of a sandwich plate can be categorized into two distinct components: extension kinetic energy and bending kinetic energy. Extension kinetic energy refers to the energy associated with the extension or stretching of the sandwich plate, arising from tensile or compressive stresses. Bending kinetic energy, on the other hand, relates to the energy associated with the bending or flexing of the sandwich plate, resulting from bending moments or transverse shear stresses.

The total kinetic energy of the MRE-based sandwich plate is the sum of the extension kinetic energy and bending kinetic energy associated with all layers. The kinetic energy of each layer, with a density denoted as ρ, is defined as:

$$T = \frac{1}{2}\rho \iiint_V \left(\left(\frac{\partial u}{\partial t}\right)^2 + \left(\frac{\partial v}{\partial t}\right)^2 + \left(\frac{\partial w}{\partial t}\right)^2\right) dV \tag{2.24}$$

The potential energy associated with a sandwich plate can be understood in terms of its deformation under external loads. When a sandwich plate is subjected to external loads, such as bending or stretching, the deformation of its constituent layers results in the storage of potential energy within the material. This potential energy is a function of the strain energy stored in the material due to its deformation.

This energy can be expressed as a sum of the energies of each layer. The potential energy corresponding to each layer consists of two parts: bending potential energy which is associated

with the deformation of the plate due to bending, and the tensile potential energy, associated with the deformation of the plate due to tensile stresses. The potential energy of each of the elastic layers (the constraining and basic layer), with the tensile and bending stresses of σ_T and σ_b , and the corresponding strain of ε_T and ε_b is calculated as:

$$V = \frac{1}{2}\iiint_V (\varepsilon_T{}^T \sigma_T + \varepsilon_b{}^T \sigma_b) dV \tag{2.25}$$

For the MRE layer, its potential energy encompasses tensile, bending, and shear strain energies, which are expressed as:

$$V = \frac{1}{2}\iiint_V (\varepsilon_T{}^T \sigma_T + \varepsilon_b{}^T \sigma_b + \gamma^T G\gamma) dV \tag{2.26}$$

where $\gamma = [\beta_x \quad \beta_y]^T$ is the shear starin of MRE layer, and *G* is the shear stiffness matrix expressed as:

$$G = \begin{bmatrix} G_x & 0 \\ 0 & G_y \end{bmatrix} \tag{2.27}$$

It should be noted that G_x and G_y represent the shear moduli in the *x* and *y* directions, respectively. However, in this research study. the MRE is treated as an isotropic material, meaning that the shear modulus is denoted as G_0, and therefore, $G_x = G_y = G_0$.

Substituting the strain energy and kinetic energy into Hamilton's principle, the governing equation for the MRE-based sandwich plate element can be derived as:

$$M^e \ddot{W}_i(t) + K^e W_i(t) = f_i \tag{2.28}$$

where, f_i represents the external force applied to the element and $M^e$and K^e are the mass and stiffness matrices of the element, defined as follows,

$$\begin{aligned} K^e &= \sum_{i=1}^{3} (K_{Ti} + K_{bi} + K_{sM}) \\ M^e &= \sum_{i=1}^{3} (m_{Ti} + m_{bi}) \end{aligned} \tag{2.29}$$

In the given equations, K_{Ti} and K_{bi} represent the extensional and bending stiffness matrices associated with the ith layer. Additionally, there is an additional term, K_{sM} , included in the stiffness matrix expression, signifying the shear stiffness matrix of the MRE layer. Furthermore, m_{Ti} and m_{bi} correspond to the extensional and bending mass matrices associated with the ith layer. The precise definitions of these matrices are provided in Appendix A. It's important to note that the shear modulus of the MRE layer, defined in Eq. (2.27), is a complex value. Consequently, the stiffness matrix of the element also becomes complex, leading to a modified equation of motion for the element:

$$M^e \ddot{W}_i(t) + ({K_R}^e + {K_I}^e)W_i(t) = f_i \tag{2.30}$$

Here, ${K_R}^e$ and ${K_I}^e$ show the the real and imaginary parts of the stiffness matrix, with the latter accounting for the damping properties of the MRE layer

Utilizing the derived stiffness and mass matrices, all elements must be assembled following standard FE procedures to achieve the complete finite element formulation for the MRE-based sandwich plate, as follows:

$$M\ddot{W} + KW = F \tag{2.31}$$

where M and K represent the assembled mass and stiffness matrices of the entire sandwich plate respectively, while F is the vector representing external forces. Additionally, W denotes the total displacement vector of the plate. Figure 2-4 illustrates the discretization view of the plate, along with the arrangement of node numbers.

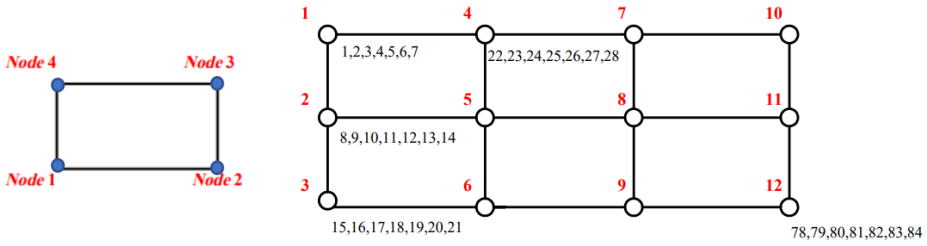

Figure 2-4: Finite element discretization of design domain

2.3.1Summary and Conclusion

In this chapter, a finite element model for the MRE-based sandwich plate under various loading and boundary conditions was developed. The proposed model utilizes rectangular elements defined by four nodes to discretize the plate. Each node is assumed to possess seven degrees of freedom. The finite element equations of motion were derived using Kirchhoff's plate theory and Hamilton's principle. In the proposed model, it was assumed that there is no slippage between the layers of the sandwich plate. Additionally, the moment of inertia of each layer was ignored, focusing solely on bending deformation for the two elastic top and bottom layers. However, for the MRE layer, both bending and shear deformation were considered.

By applying the proposed finite element model, the vibration and damping characteristics of the MRE-based sandwich plate can be analyzed numerically. This analysis allows us to understand how the plate behaves under various loading conditions and boundary constraints. These insights are crucial for optimizing the layout of the MRE layer, a topic that will be explored in the next chapter.

Chapter 3: Topology optimization

3.1 Introduction

This chapter focuses on the development of topology optimization formulation to identify the optimal material distribution within a given domain.

Structural optimization involves determining the optimal material distribution within a defined physical volume domain to effectively transmit applied loads while adhering to constraints set by the manufacturer and intended usage. This process usually involves mathematical modeling, simulation, and iterative analysis guided by optimization algorithm. It commences with defining the design space, which is the area where material can be allocated. Subsequently, design variables, such as material densities or thicknesses, are introduced to represent material distribution within this design space. Constraints are then imposed to ensure that the optimized design meets specific requirements and limitations. Structural optimization problems can be categorized into three types: sizing, shape (layout), and topology optimization [51]. Examples of each type are clearly illustrated in Figure 3-1.

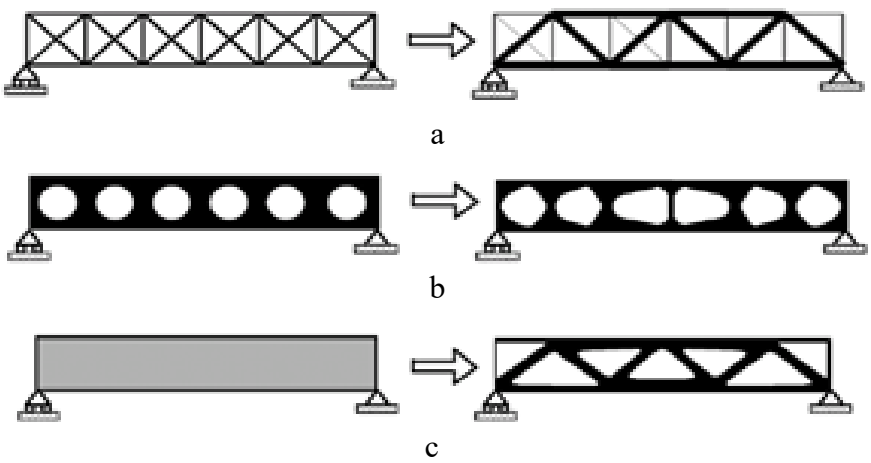

Figure 3-1: Examples of (a) Size Optimization, (b) Shape Optimization and (c)Topology Optimization [51]

Size optimization mainly aims to find the most efficient dimensions for a structure, like trusses and bridges, considering the loads they need to support. It typically involves analyzing the bars or members making up the structure to determine the best dimensions and shapes for each member, to ensure optimal performance. In size optimization the layout of the layout or shape of the

structure is not changed and no member is removed. For instance, in truss structures shown in Figure 3-1(a), the size optimization involves identification of optimal cross-sectional area of the bar members.

In shape optimization, the focus is on refining the design parameters of a structure, such as fillets, chamfers and radiuses to meet specific performance requirements while satisfying various design constraints. Nodal coordinates on the boundaries are generally design variables in layout optimization. For instance, in Figure 3-1(b) the nodal coordinates in the perimeter of internal circular holes are considered design variables.

Topology optimization employs mathematical algorithms and computational techniques to optimize the distribution of materials within a designated design domain while meeting specific design criteria, including load-carrying capacity, stiffness, and material volume. The optimization algorithm iteratively modifies the topology of the design space by adding or removing material, as shown in Figure 3-1 (b), from each element until it reaches an optimal configuration. Through the optimization of material distribution within a design domain, topology optimization can decrease material consumption, reduce weight and cut manufacturing expenses, while enhancing the performance and durability of the final design.

Topology optimization finds widespread application in industries such as aerospace, automotive, and mechanical engineering, where weight reduction and high-performance design are of paramount importance. However, its application is not confined to these sectors and is extending to other domains such as architecture and medical devices.

Certainly, the optimization process may yield designs that are not immediately implementable due to practical constraints such as manufacturing limitations, cost considerations, or other factors. Nevertheless, these optimized designs provide valuable insights for the design process, enabling engineers and designers to evaluate more feasible designs and continue refining the optimization process.

In topology optimization, the design space can be either a continuum or a discrete structure. Continuum structures are typically composed of solid materials and exhibit continuous properties,

while discrete structures are typically consist of elements like beams, trusses, or plates that are interconnected at discrete points.

3.2 Topology Optimization Methods

There are various approaches to implement topology optimization. According to Sigmund [52], five different major optimization approaches have been developed over time. Those approaches include, methods of topological derivative, phase field method, evolutionary technique, level set method and density approach [53].

The topological derivative method is a mathematical approach employed for optimizing structures by predicting the effects of small holes introduced within the design domain. This method was introduced in 1994 by Eschenauer [54] and was initially referred to as the bubble method. The fundamental concept behind this method is to initiate optimization by introducing a small hole within the design domain. This small hole serves as a starting point for generating larger openings. Mathematical techniques are employed to predict the impact of this small hole on the entire structure, and this information is then utilized to create new openings, optimizing the structure further [54]. The use of topological derivatives in conjunction with other optimization methods has been found to be effective in solving engineering problems. Sigmund [52] suggested that in 2D scenarios, combining topological derivatives with level set methods is necessary to develop the optimum topology.

The phase field method is an approach that is directly dealing with the density variables. To find the optimal distribution of material, the phase field method employs gradient-based optimization algorithms. These algorithms iteratively update the phase field variable to minimize or maximize the objective function. They rely on the gradient of the objective function with respect to the design variable to guide the optimization process.

The evolutionary method was first introduced in 1993 for structural optimization, known as Evolutionary Structural Optimization (ESO) at that time. ESO is a structural optimization technique that uses an evolutionary algorithm to optimize the design of a structure by iteratively removing parts of the structure, considering the defined rejection criterion, until a desired level of performance is achieved. This method belongs to the category of well-known discrete optimization methods, which are highly sensitive to changes in the design parameters [52].

The level set method, initially developed by Osher and Sethian in 1988 [56], mainly focuses on defining the boundary of an object using a zero-level contour of the level set function. [53].

The density approach was first developed by Bendsøe in 1989 [57]. Among various topology optimization approaches, the most widely adopted method is the density-based approach [58].

In this research study , a density-based topology optimization has been formulated. In this method, the material distribution is represented by a discretized domain, where each element corresponds to a design variable representing material density. Structural response, necessary for optimization, is typically computed using the finite element method, which also relies on domain discretization [59]. In this context, the domain discretization used for density interpolation and finite element analysis is identical.

In theory, density can be represented as either zero or one, indicating the presence or absence of material in an element. However, this discrete approach is not suitable for many optimization methods. To address this issue, the density-based optimization approach is implemented to relax the optimization problem form the binary, on-off nature of the problem by defining a continuum density ranging between zero and one [61,63]. For example, Figure 3-2 illustrates the outcome of applying the density-based topology optimization approach to the MBB-beam problem.

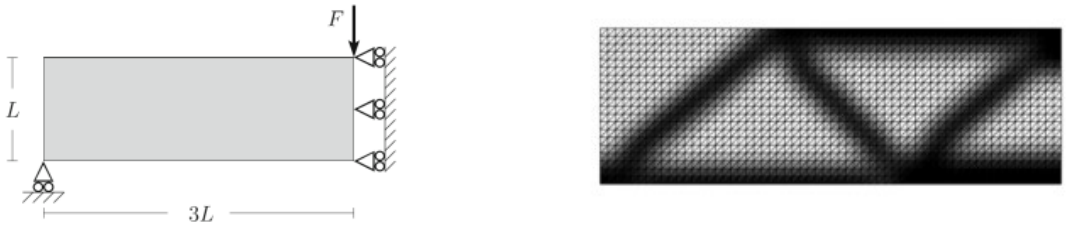

a)The schematic view of MBB-beam problem b)Density-based topology optimization result

Figure 3-2: Typically density-based topology optimization result [61]

3.3 Material Properties Interpolation

In the density-based optimization approach, the material properties of each element in the discretized domain are related to their density by applying a power-law interpolation function [60]. One of the methods used for the material interpolation scheme is SIMP method [62]. The SIMP

approach is widely regarded for its conceptual and practical simplicity and has proven successful in many applications [63], [64], [65], [66]. This approach involves discretizing the design domain into small elements and assigning a design variable (the element density) to each element. Also, it assumes that the material properties within each element are constant and isotropic [67]. For intermediate densities (i.e., densities between 0 and 1), the SIMP approach penalizes these intermediate densities using a penalization factor to achieve better binary topology patterns. Applying this method, Young's modulus is interpolated as a function of the material density using an artificial model, as follows:

$$\rho(x_e) = x_e \rho_{x_e=1}$$
$$E(x_e) = (x_e)^p E_{x_e=1} \tag{3.1}$$

where x_e is the relative density of each element and p is the penalization factor.

However, for the studied model here, as the damping properties of the MR layer is of high importance in mitigating the vibration which is the main objective, shear modulus of MRE layer is interpolated based on the SIMP method. This has resulted to the development of MREP model in which the shear modulus G, and the material density ρ of each MRE element are respectively defined as:

$$G(x_e) = (x_e)^p G_{x_e=1}$$
$$\rho(x_e) = x_e \rho_{x_e=1} \tag{3.2}$$

the value of the penalization factor p depends on the problem generally, although the value of 3 is reported to provide a satisfactory solution [52].

Applying the above material interpolation and referring to finite element modelling of the structure, one can obtain the following expressions for the stiffness and mass matrix of the MR layer elements:

$$K(x_e) = (x_e)^p K_{x_e=1}$$
$$M(x_e) = x_e M_{x_e=1} \tag{3.3}$$

It is noted that, $K_{x_e=1}$ and $M_{x_e=1}$ are the stiffness and mass matrix of the full coverage MRE layer elements.

3.4 Optimization Problem Formulation

To formulate the optimization problem effectively, it is essential to define a suitable objective function that ensures the best performance of the structure in reducing the vibration level. In harmonic vibration problems, one of the most commonly used objective functions is dynamic compliance, first introduced by Ma et al. [69] and initially defined as an extension of the concept of compliance used in static problems [70].

The dynamic compliance of a sandwich plate, denoted as *f*, for a discretized domain is calculated as:

$$f = U^T F \tag{3.4}$$

where *F* represents the loading vector of the nodes, and *U* is the vector of DOFs of the nodes. Obviously, applying a full coverage of MRE layer would be the most effective design for reducing vibration levels in the sandwich plate. However, many practical applications necessitate weight constraints on the system. Consequently, in this study, a material volume constraint is introduced into the optimization problem for implementing the weight restriction. Taking this constraint into account, the optimization problem for a MRE-based sandwich plate under a harmonic loading with frequency ω is defined as:

$$\begin{aligned} & Min\ f(x) \\ Subject\ to \begin{cases} & (K - \omega^2 M)U = F \\ & \sum_{i=1}^{N_e} x_i V_i \le V_0 \\ 0 \le x_i \le 1 \quad & i = 1,2,3,\dots,N_e \end{cases} \end{aligned} \tag{3.5}$$

In this formulation, *M* and *K* represent the mass and stiffness matrices of the plate. The optimization problem variables are the density of the MRE layer in each element, denoted as the vector *x*, within a domain discretized with N_e number of elements. Here, $x_i = 0$ and $x_i = 1$ correspond to void and solid elements considering the MRE layer, respectively.

Additionally, the symbol V_i represents the volume of an element with full coverage of the MRE layer, while V_0 denotes the allowable volume fraction, which imposes a mass restriction on the plate.

3.4.1Optimization Algorithm

There are various gradient based optimization algorithms, such as sequential linear programming (SLP) and sequential quadratic programming (SQP), used to find solutions for optimization problems. Among these methods, the method of moving asymptotes (MMA) is notably powerful, especially in terms of solving multi variable and multi constraints optimization problems. MMA offers improved convergence by considering two past successive iterations during the optimization process [36].

3.4.2The Method of Moving Asymptotes

The method of moving asymptotes (MMA), introduced by Svanberg in 1987 [72], remains the most widely used among sequential approximation methods in the field of structural topology optimization [73]. MMA is a general-purpose algorithm suitable for various optimization problems [74, 75]. Due to its basis in convex approximation, it's suitable for topology optimization, however its efficiency is strongly influenced by asymptote and move limits [75].

In this method, the optimization problem is defined as [74, 36]:

$$\begin{aligned} &Minimise \quad f_0(X) + a_0 z + \sum_{i=1}^{m} \left(c_i y_i + \frac{1}{2} d_i {y_i}^2 \right) \\ &Subject\ to \quad f_i(X) - a_i z - y_i \leq 0 \qquad i = 1,2,\ldots\ldots,c \\ &\qquad\qquad x \in X, \qquad y \geq 0, \qquad z \geq 0 \end{aligned} \tag{3.6}$$

where, $f_0(X)$ is the cost function to be minimized and X is the vector of design variables, y and z are artificial optimization variables, c is the number of constraints and a_0, a_i, c_i and d_i are the constant coefficients. The choice of these coefficients allows for the adaptation of Eq. (3.6) to various optimization problems. As explained by Svanberg [74], setting $a_0 = 1$ and a_i=0 for all i,

then $z = 0$ in any optimal solution, and by considering $d_i = 0$ and c_i= "a large number," then the variables $y_i = 0$ for all i, the optimization problem defined in Eq. (3.6) will be matched to the optimization problem stated in Eq. (3.5). To solve the optimization problem, the external MMA code provided by in Ref [36] has been used. The flowchart of the proposed topology optimization algorithm is shown in Figure 3-3.

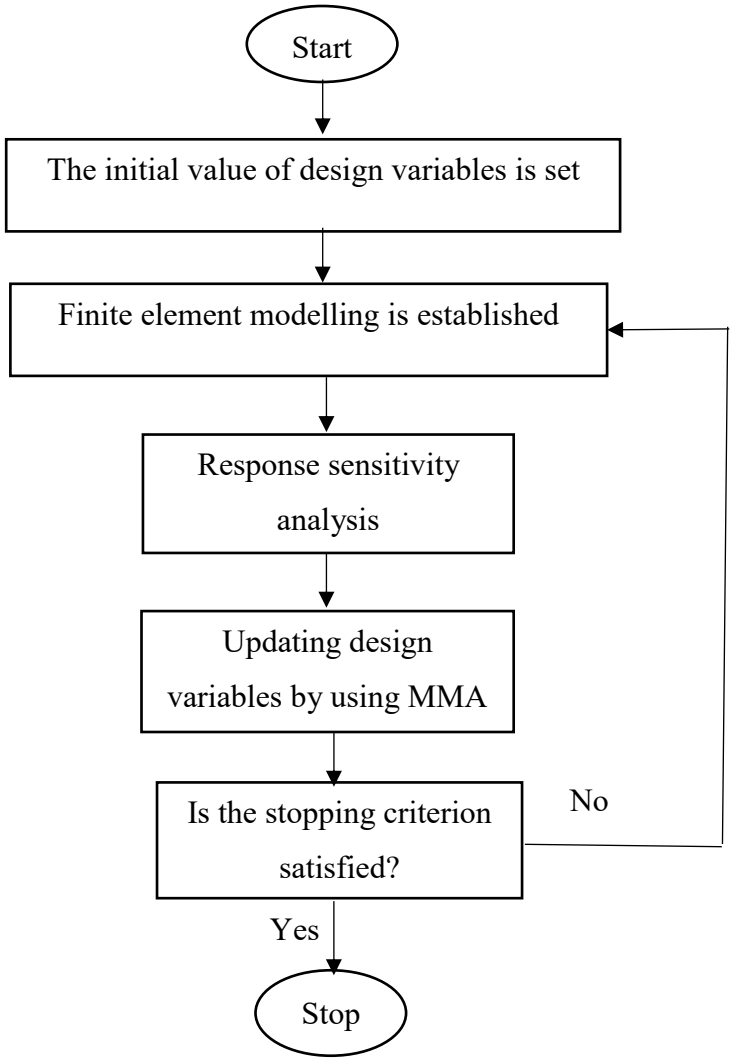

Figure 3-3: Flowchart of the proposed optimization method

As depicted in the flowchart above, performing the MMA necessitates the implementation of sensitivity analysis for the objective function, specifically the dynamic compliance. Given the complex nature of the stiffness matrix and the displacement vector, the dynamic compliance is defined as:

$$C = U^T F = \left({U_R}^T + {U_I}^T i\right)\left({K_R}^T + {K_I}^T i - \omega^2 M\right)(U_R + U_I i) \tag{3.7}$$

where, U_R and K_R represent the real parts of the stiffness matrix and displacement vector, while U_I and K_I represent their respective imaginary parts.

Using Eq. (3.7) and applying the chain rule, the sensitivity of dynamic compliance with respect to the design variable x_i is expressed as [75]:

$$\begin{aligned}
&\frac{\partial |C|}{\partial x_j} = \frac{1}{|C|}\left(C_R \frac{\partial C_R}{\partial x_j} + C_I \frac{\partial C_I}{\partial x_j}\right) \\
&\frac{\partial C_R}{\partial x_j} = {u_R}^T\left(\frac{\partial K_R}{\partial x_j} - \omega^2 \frac{\partial M}{\partial x_j}\right)u_R - {u_R}^T\left(\frac{\partial K_I}{\partial x_j}\right)u_I - {u_I}^T\left(\frac{\partial K_R}{\partial x_j} - \omega^2 \frac{\partial M}{\partial x_j}\right)u_I - {u_I}^T\left(\frac{\partial K_I}{\partial x_j}\right)u_R \\
&\frac{\partial C_I}{\partial x_j} = {u_R}^T\left(\frac{\partial K_R}{\partial x_j} - \omega^2 \frac{\partial M}{\partial x_j}\right)u_I + {u_R}^T\left(\frac{\partial K_I}{\partial x_j}\right)u_R + {u_I}^T\left(\frac{\partial K_R}{\partial x_j} - \omega^2 \frac{\partial M}{\partial x_j}\right)u_R - {u_I}^T\left(\frac{\partial K_I}{\partial x_j}\right)u_I
\end{aligned} \tag{3.8}$$

Referring to Eq. (3.3), the following expressions are derived for the derivatives of the stiffness and mass matrices:

$$\begin{aligned}
&\frac{\partial M}{\partial x_j} = M_{x_e=1} \\
&\frac{\partial K}{\partial x_j} = p(x_e)^{p-1} K_{x_e=1}
\end{aligned} \tag{3.9}$$

3.5 Summary and Conclusion

Topology optimization is a powerful technique used to determine the optimal distribution of material within a given domain. In this chapter, the focus is on investigating topology optimization, specifically the density-based approach, which is widely used. The density-based approach represents the material distribution using a discretized domain, where each element is associated with a design variable representing the material density. In this particular study, the material properties of the domain elements are interpolated using the SIMP approach. SIMP is a popular method for representing material properties in topology optimization. In this case, the SIMP approach is extended to include magnetorheological elastomer properties, resulting in the developed MREP model.

The optimization algorithm employed in this study is the method of moving asymptotes (MMA). MMA is utilized to update the optimization variables in each iteration of the topology optimization process. This algorithm helps in iteratively improving the material distribution within the domain to achieve the desired objective.

The objective function in the optimization method is defined as the dynamic compliance of the plate under various loadings. By minimizing the objective function, the vibration level of the plate is reduced. The goal of the topology optimization process, in this case, is to find the material distribution that minimizes the dynamic compliance and hence optimizes the plate's vibration characteristics.

Through the application of the density-based topology optimization approach, utilizing the MREP model, and employing the MMA algorithm for optimization, this study aims to determine the optimal material distribution within the domain to reduce the vibration levels of the plate under different loadings.

Chapter 4: Results and Discussion

4.1 Introduction

This research study aims at the development of design optimization to identify the optimal topology of the MR layer within a sandwich plate, composed of an MR elastomer layer between two elastic plates. The dynamic response of the structure subjected to harmonic loading is achieved using the finite element method. The objective is to minimize dynamic compliance to enhance vibration control capabilities. The SIMP method is extended, introducing the developed MREP model for material properties interpolation. The optimization problem is solved using MMA method, which relies on a specialized convex approximation [19]. To validate the proposed method, detailed numerical examples are presented in this chapter. These examples demonstrate the effectiveness of the developed approach in identifying the most efficient topologies of MRE layer for vibration reduction in sandwich structures.

4.2 Finite Element Model Validation

In this section, the validity of the developed finite element code executed in the Matlab environment is examined by considering a rectangular MRE-based sandwich plate. The MRE based sandwich plate is simply supported in all four edges and its properties are based on those used by Yeh et al. [76] which are breifly summarized in Table 4-1.

Table 4-1: Mechanical properties of the sandwich plate [76]

Top and bottom layers	Young's modulus	70 Gpa
	Poison's ratio	0.3
	Mass density	2700 kg/m^3
	Constraining layer thickness	0.000375 m
	Base layer thickness	0.00125 m
MRE layer	Thickness	0.000625 m
	Mass density	3500 kg/m^3
Structure size	Length	0.3 m
	Width	0.2 m

The validity of the FE model is assessed by comparing the obtained responses, specifically the natural frequencies, with those reported by other researchers. Table 4-2 provides results for the first four frequencies under two different values of the average magnetic flux density (200 and 400 G). As it can be realized, results are in very good agreement with those obtained by Yeh [76] and Zhang [77] who also used FE method to determine the vibration characteristics of the sandwich plate.

Table 4-2: Comparisons of the first four natural frequencies (Hz) of the MRE sandwich plate under two different magnetic flux densities

Magnetic flux density (200G)					
Natural frequency	Present study (Hz)	Yeh et.al [76] (Hz)	Error%	Zhang et.al [77] (Hz)	Error%
First	108.28	107.34	0.88	109.39	1.02
Second	188.08	183.81	2.32	188.26	0.10
Third	284.04	283.06	0.35	283.67	0.13
Fourth	314.18	313.09	0.12	313.97	0.07
Magnetic flux density (400G)					
Natural frequency	Present study (Hz)	Yeh et.al [76] (Hz)	Error%	Zhang et.al [77] (Hz)	Error%
First	113.74	115.01	1.10	115.32	1.37
Second	197.14	195.21	0.98	197.03	0.06
Third	295.60	296.21	0.206	294.70	0.30
Fourth	326.95	327.15	0.06	325.49	0.45

4.3 **Topology Optimization Validation**

In this section, the accuracy of the proposed optimization approach is investigated. To do so, a rectangular MRE-based sandwich plate with properties similar to those studied by Zhang et al. [77] is considered. In their study, the goal was to obtain the optimal layouts of MR fluid layer. To achieve this, an optimization problem was formulated with the dynamic compliance of the sandwich plate as the objective function while incorporating a mass constraint. To solve the optimization problem, they applied the globally convergent method of moving asymptotes (GCMMA), a powerful gradient-based mathematical programming algorithm. The material properties of the base layer and the constraining layer, as well as the structural dimensions, are the same thosein Table 4-1. For the MR fluid layer, the density is 3500 kg/m^3, and for the sealant

material, the Young's modulus, Poisson's ratio, density, and thickness are 0.22 GPa, 0.4, 1233 kg/ m^3, and 0.1 mm, respectively. The plate is simply supported at all edges and subjected to concentrated harmonic loading applied at the middle of the plate. Figure 4-1 illustrates a comparison of the optimum topologies for the plate under a magnetic field of 200 G and a loading magnitude of 1000 N at different frequencies. It is worth noting that, to the best of our knowledge, there is no study on the topology optimization of MRE layer in MRE-based sandwich plates. Thus, for the validation purposes instead the available results for topology optimization of MR fluid-based sandwich plate reported by Zhang et al. [77] were used.

It should also be noted that the developed topology optimization code defines two stopping criteria. The first is the classical criterion, which considers the density change between two successive iterations. The second criterion is based on the maximum number of iterations. Optimization will stop when either of these criteria is satisfied. The reason for introducing the second criterion is that the density change alone may not effectively stop the optimization process, or it may require a very high number of iterations, even when there are no significant oscillations in the objective function's value.

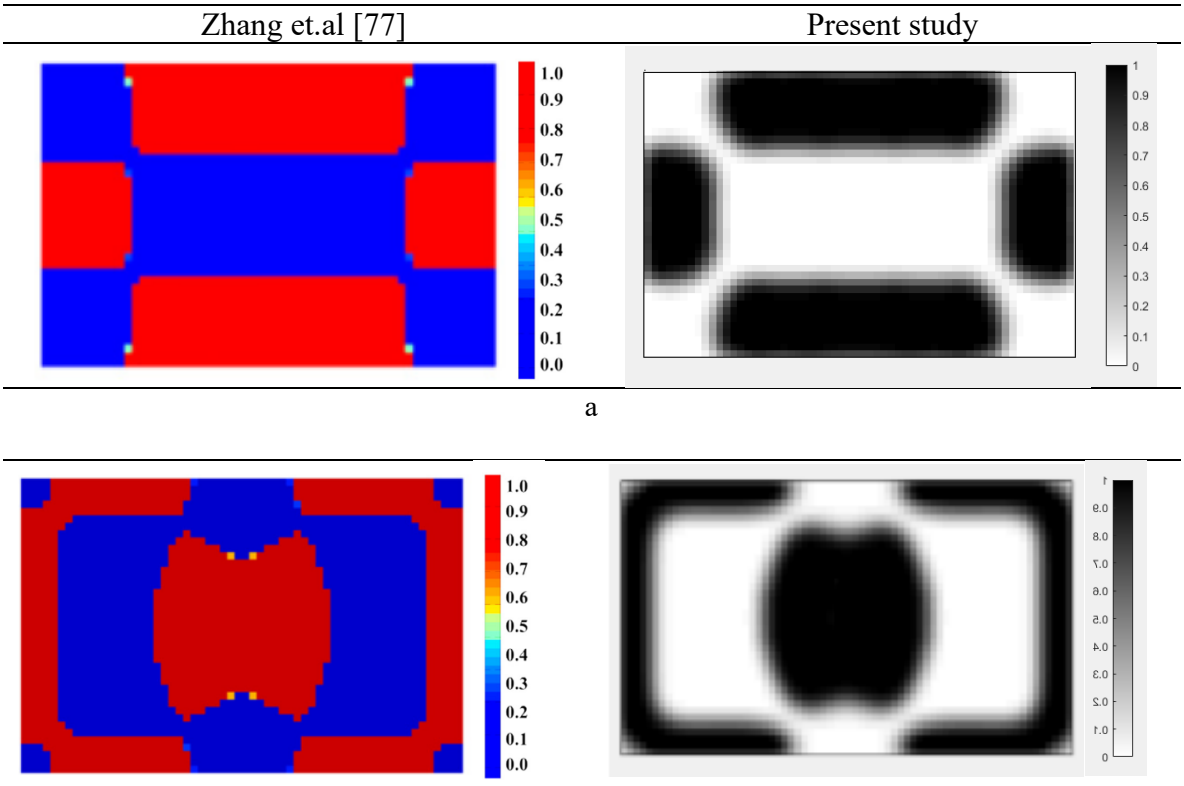

a

b

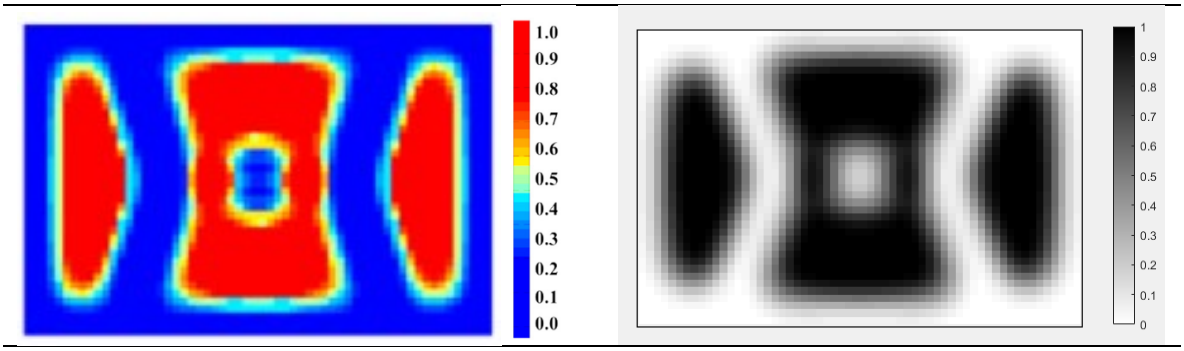

c

Figure 4-1: Comparisons of the Optimization results for MR fluid layers obtained from the model and other literature data under different excitation frequencies. (a) 80 Hz; (b) 280 Hz ; (c) 400 Hz

Figure 4-1 illustrates a reasonably good agreement between the results for all frequencies, indicating the high accuracy of the proposed optimization method.

4.4 Topology Optimization Examples

In this section, the validated analysis and optimization methods are effectively used to investigate the optimal topologies of the magnetorheological elastomer (MRE) core layer in MRE-based sandwich plates under various boundary and loading conditions including CFCF (two edges are clamped and the other two are free) and SSSS (all edges are simply supported) and CFFF (clamped at one edge and free at other sides). In all the investigated examples, the plate is subjected to a magnetic field of 200G. The geometric boundary conditions for the clamped and simply supported edges are given, such that:

$$\begin{aligned} &Clamped && u_c = v_c = u_b = v_b = w = \theta_x = \theta_y = 0 \\ &Simply\ supported && w = 0 \end{aligned} \tag{4.1}$$

4.4.1Simply Supported Plate (SSSS)

A sandwich plate, with MRE embedded between two aluminum plates as shown in Figure 4-2, is considered. The properties of the plate are summarized in Table 4-3. The plate is assumed to be simply supported at all four ends under a time-harmonic external force ($F = f_0 e^{i\omega t}$), where f_0 is the magnitude and ω the frequency of the loading. In this example, this point force is applied at the center of the plate with the dimensions of $L_1 = 0.35$ m and $L_2 = 0.2$ m.

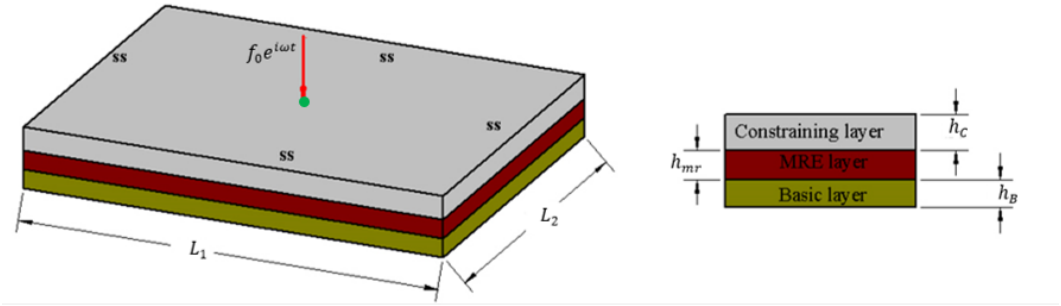

Figure 4-2: MRE-based sandwich plate (SSSS) under harmonic loading applied at the center

Table 4-3: Mechanical properties of the sandwich plate

Top and bottom layers	Young's modulus (E_C, E_B)	70 Gpa
	Poison's ratio (v_C, v_B)	0.3
	Mass density (ρ_C, ρ_B)	2700 kg/m^3
	Constraining layer thickness (h_C)	0.0004 m
	Base layer thickness (h_B)	0.002 m
MRE layer	Thickness (h_{mr})	0.0004 m

Considering the MRE core with a 25% volume fraction of carbonyl iron particles (CIPs), the core density would be 2771 kg/m³. Assuming that the MRE core layer operates in the linear viscoelastic region, the complex shear modulus G of the viscoelastic layers can be written as:

$$G = G' + iG'' \tag{4.2}$$

where, G' and G'' represent the storage and loss moduli of the MRE material which can be varied under the application of an external magnetic field.

For the considered MRE, the storage modulus can be determined as a polynomial function of the magnetic field intensity B (in Tesla) as reported in [78]:

$$G'(B) = -1283B^4 + 1904B^3 - 271.2B^2 + 73.84B + 55.19\ [kPa] \tag{4.3}$$

It is worth noting that, for the mentioned MRE, the storage modulus changes significantly upon the application of a magnetic field, while the change in the loss factor can be considered negligible at approximately 0.145 [78]. So, the loss moduli can be easily determined.

To implement the finite element method, the convergence history of the dynamic compliance is analyzed to determine the optimal number of elements required for meshing the plate, as depicted in Figure 4-3. This figure illustrates how dynamic compliance changes as the number of elements in the mesh increases. A penalty factor, p, equal to 3 is adopted. The applied force has a magnitude of 1000 N and a frequency of 150 Hz. Additionally, the MRE mass is allowed to be half of the mass in the full coverage case, corresponding to a volume fraction of 0.5 with the design variables set to ($x_i = 0.5$).

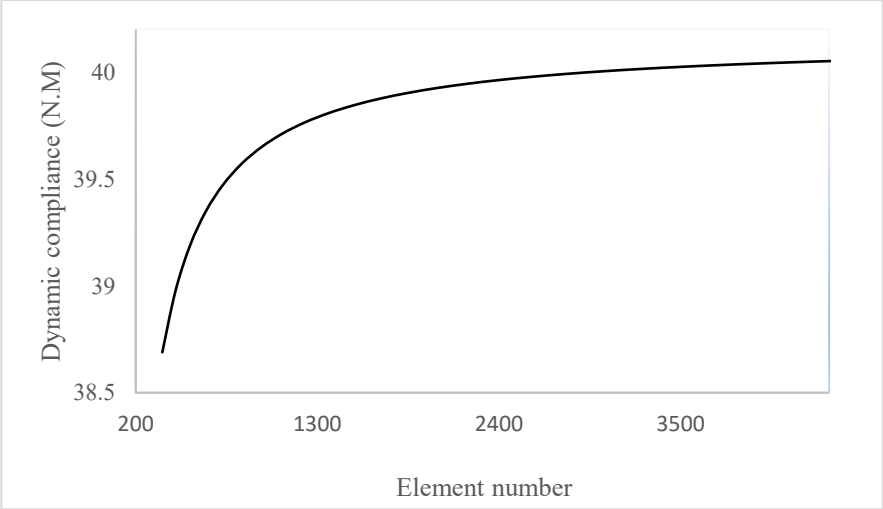

Figure 4-3: Convergence history of dynamic compliance

Referring to Figure 4-3, the finite element method is implemented with 3500 elements, resulting in a grid of (70×50) elements and 24500 degrees of freedom. This number of elements is chosen as further increasing the number of elements will have no noticeable effect on dynamic compliance.

The optimization process begins with the initial values of the design variables set to ($x_i = 0.5$). The penalty factor for the model is chosen as p = 3. The applied force has a magnitude of 1000 N and a frequency of 150 Hz.

The optimization process history for the dynamic compliance and volume fraction are shown in Figure 4-5 suggesting rapid converge of the topology optimization algorithm.

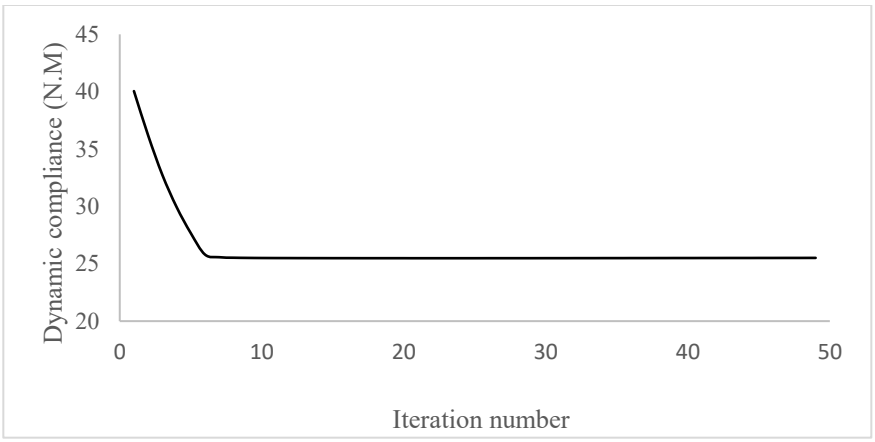

a

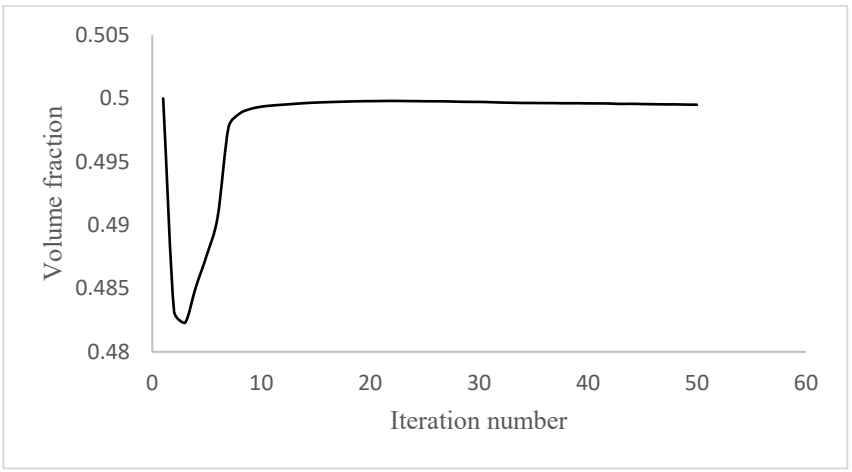

b

Figure 4-4: Optimization process history of the MRE sandwich plate (SSSS): a) Convergence history of the dynamic compliance, b) Convergence history of the volume fraction

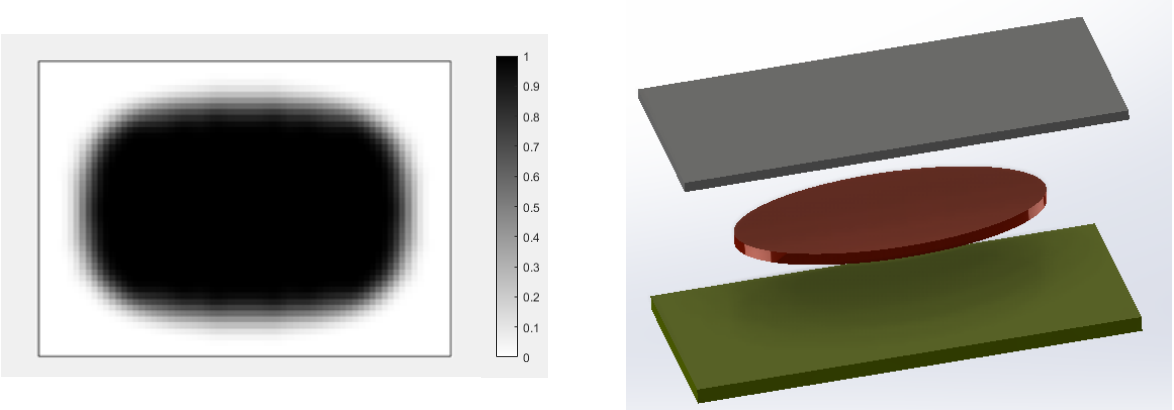

Figure 4-5: Optimal distribution of MRE layer for the MRE sandwich plate (SSSS) under the excitation frequency of $\omega = 150$ Hz

Final optimal topology of the MRE layer is shown in Figure 4-4. As depicted in Figure 4-3, the dynamic compliance has decreased by 36.29% from f = 40.05 N·m at initial configuration to f = 25.51 N·m at the final optimum solution. The effectiveness of the obtained optimum topologies in reducing vibration level is compared with an arbitrary case shown in Figure 4-5 in which the entire MRE has bee placed in one half of the plate (considering 50% volume fraction constraint on MRE). Results for vibration amplitude at all nodes are shown in Figure 4-6 for the deflection of the nodes. It is noted to that the numbering of nodes and their arrangements are based on the scheme shown in Figure 2-4. It should also be note that for the better demonstration and to include all nodes in Figure 4-7, the domain has been discretized using (30×20) elements. The results clearly show that the optimal topology configuration significantly reduces the vibration amplitude compared with the MRE layout shown in Figure 4-6.

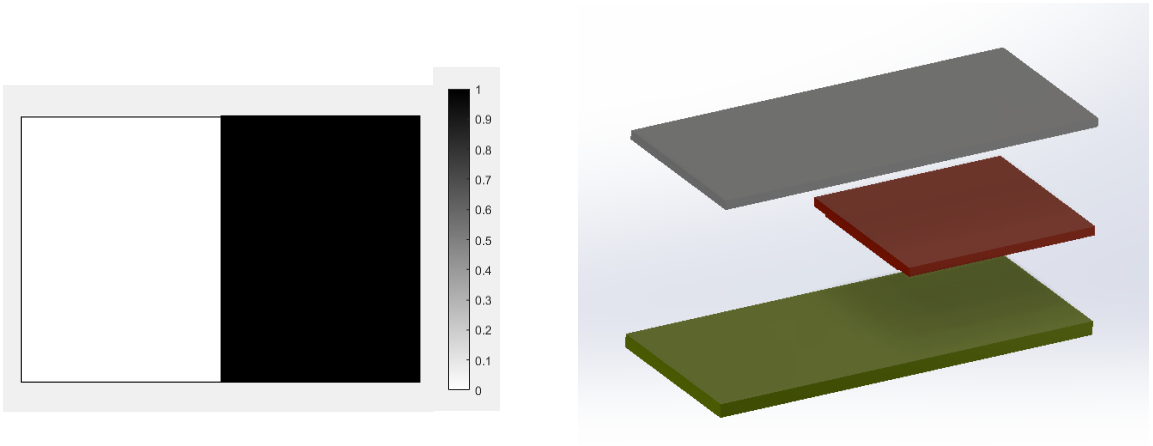

Figure 4-6: MRE distribution for an arbitrary case in the MRE sandwich plate (SSSS)

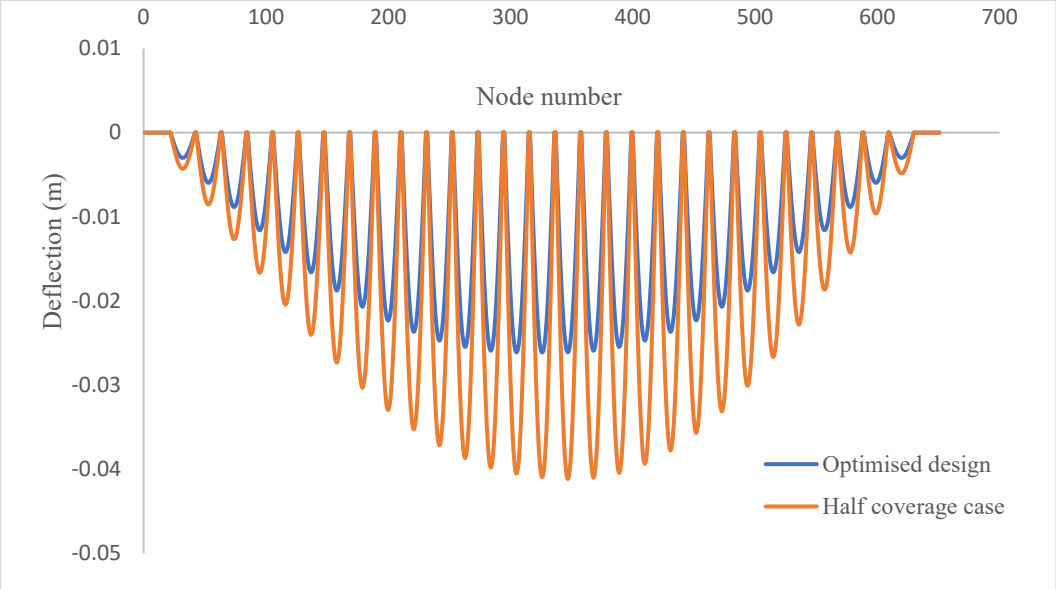

Figure 4-7: Optimal distribution of MRE layer for the MRE sandwich plate (SSSS) under the excitation frequency of $\omega = 150$ Hz

4.4.2 Clamped-clamped Plate (CFCF)

In this example the optimal topology of the MRE layer in a square plate clamped at both ends (Figure 4-7) is investigated. The properties of the constraining and basic layers, as well as the MRE layer, are the same as those presented in Table 4-3. The plate has dimensions of $L_1 = L_2 = 0.5$ m and is considered under different harmonic loadings at three different points of A, B and D as shown in Figure 4-7.

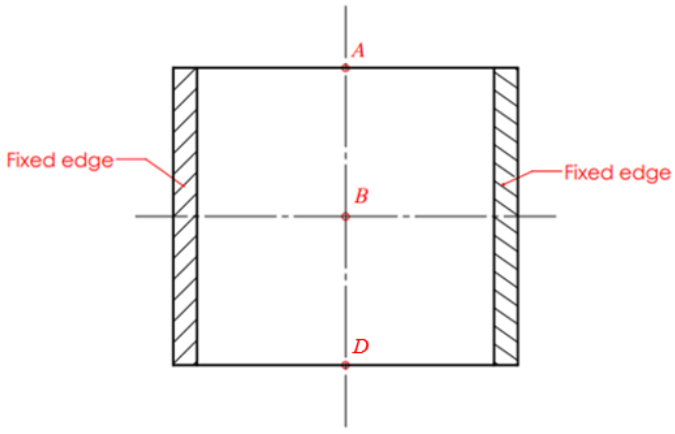

Figure 4-4: Clamped-clamped MR sandwich plate with loading positions of A.B and D

Four different cases have been investigated as described below. It is worth nothing that for all of these cases, the plate is discretized using (60×60) elements.

Case I: In the first case, the MRE sandwich plate (CFCF) is under two concentrated harmonic loadings at the middle point (Point B) and one end point (Point A), with a magnitude of 1000 N and a frequency of 280 Hz as shown in Figure 4-8.

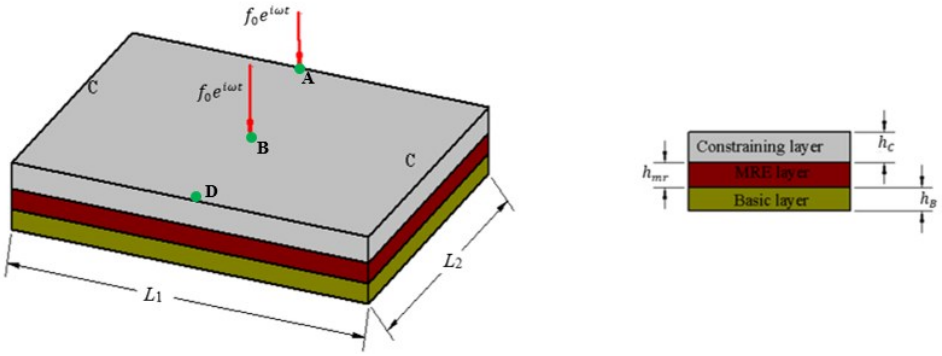

Figure 4-5: MRE sandwich plate (CFCF) with loading positions at A and B (Case I)

For this case, the iteration history for the dynamic compliance and volume fraction is shown in Figure 4-9. In this example, maximum volume fraction of the MRE is set at V_0=50% with the initial values of the design variables set to ($x_i = 0.5$). Figure 4-9 illustrates that the dynamic compliance has decreased by 34.77%, from $f = 6.50\ \mathrm{N.m}$ for the initial distribution to $f = 4.24\ \mathrm{N.m}$ for the optimum topology configuration.

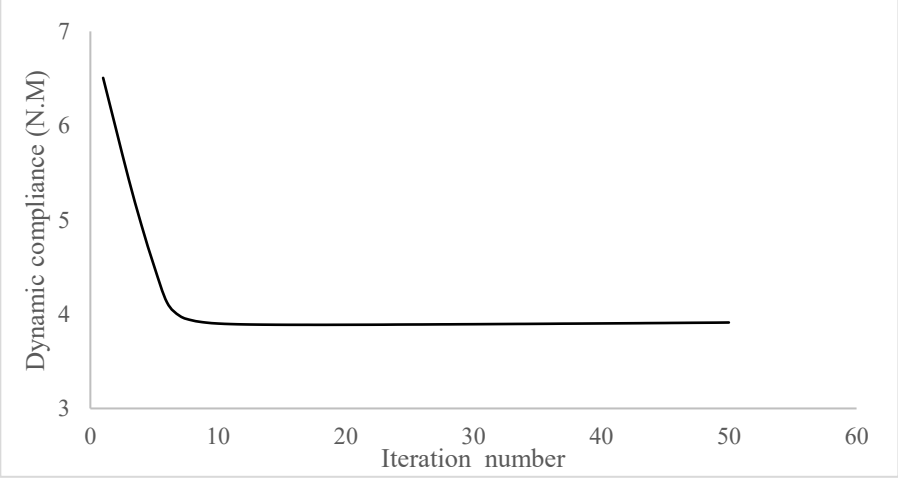

a

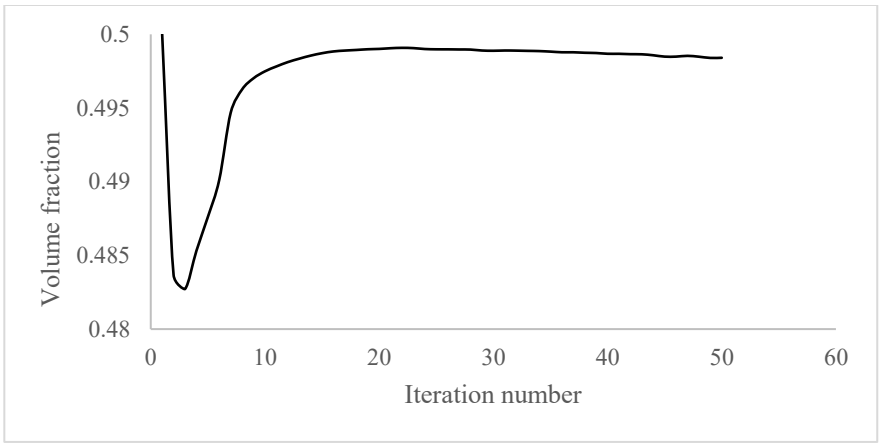

b

Figure 4-6: Optimization process history of MRE sandwich plate (CFCF): a) Convergence history of the dynamic compliance, b) Convergence history of the volume fraction (Case I)

The effect of volume fraction constraint on the optimum topology of the MRE has also been investigated and results for the volume fractions of 0.1, 0.3, 0.5, 0.7 are shown in Figure 4-10.

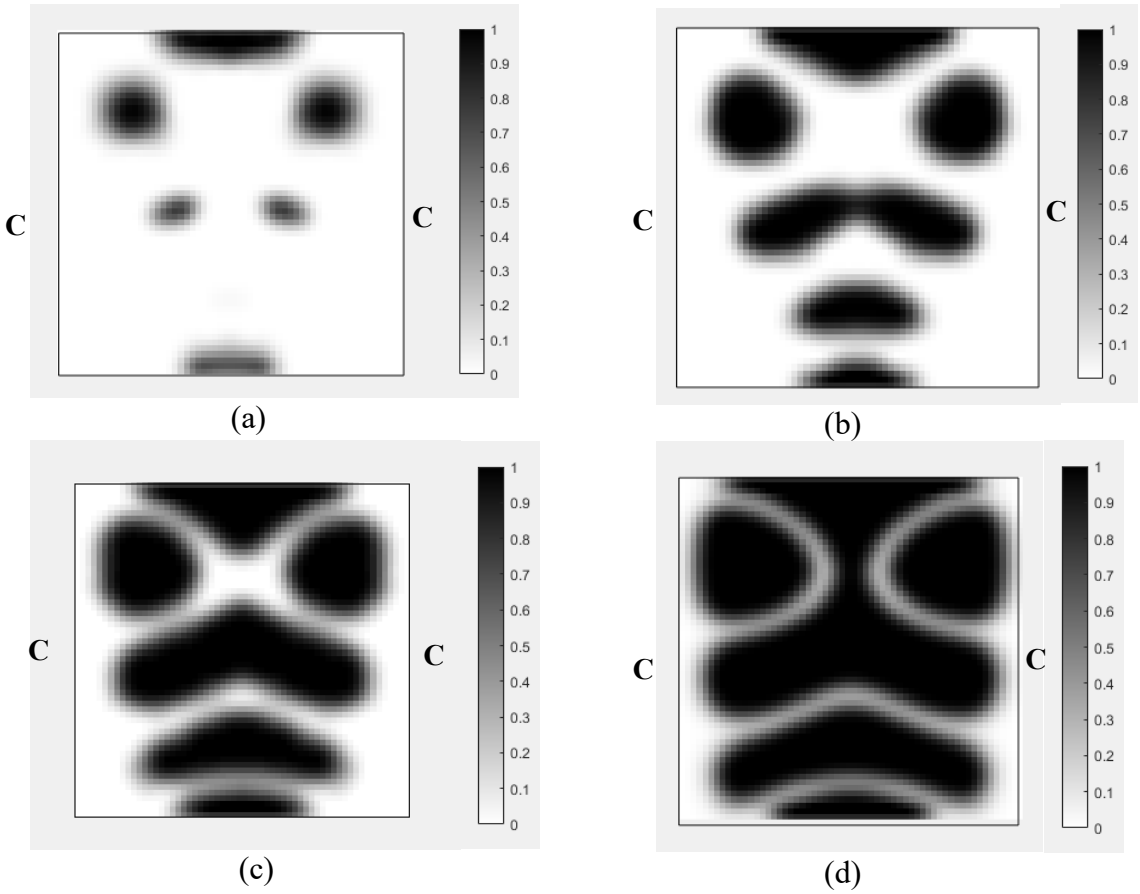

Figure 4-7: Optimal topology of the MRE layer for MRE sandwich plate (CFCF) under different volume constraints: a) 0.1; b) 0.3 c) 0.5 d) 0.7 (Case I).

The optimum objective functions at the aforementioned volume fractions are given in Table 4-4. It is interesting to note that relatively slight reduction in optimum dynamic compliance has been achieved (14%) by increasing volume fraction from 0.3 to 0.5 (60%).

Table 4-4: The effect of volume fraction constraints on optimum dynamic compliance for MRE sandwich plate (CFCF) for Case I.

Volume fraction	Optimum dynamic compliance (N.m)
0.1	7.70
0.3	4.95
0.5	4.24
0.7	3.50

The effect of loading excitation frequency on the optimum topology of the MRE sandwich plate is also investigated and results are shown in Figure 4-11. It is noted that the magnitude of the applied forces is kept at 1000 N.

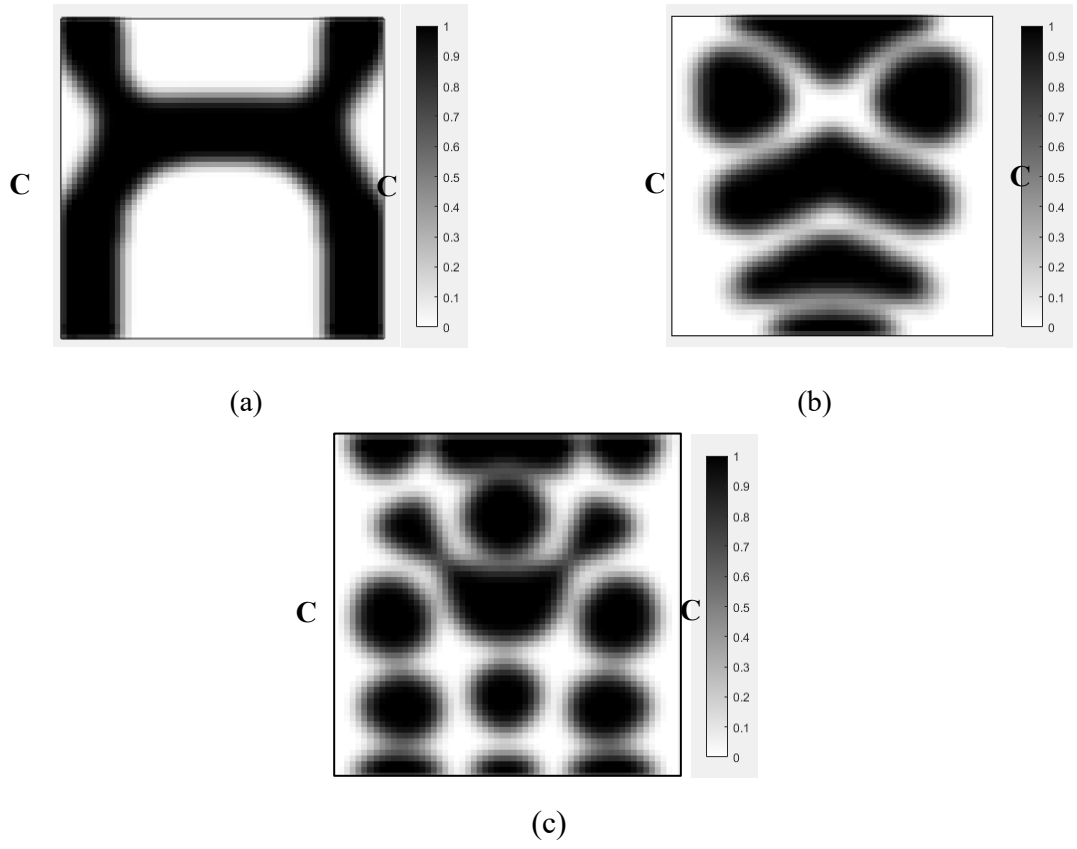

(a) (b)

(c)

Figure 4-8: Optimal topology of the MRE layer MRE sandwich plate (CFCF) under different loading frequency: a) 45 Hz; b) 280 Hz; c) 440 Hz (Case I)

Case II: In this case, the MRE sandwich plate (CFCF) is under three concentrated harmonic loadings at points A, B and D as shown in Figure 4-12 with a magnitude of 1000 N and a frequency of 280 Hz similar to Case I.

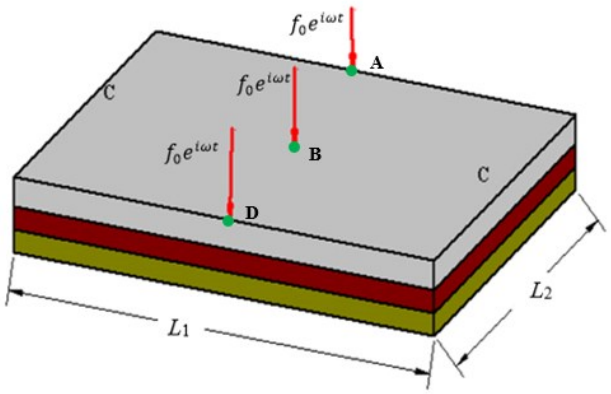

Figure 4-9: MRE sandwich plate (CFCF) with loading positions at points A, B and D (Case II)

Similar investigation has been conducted for this case and the developed topology optimization algorithm rapidly converged to the optimum solution as shown in Figure 4-13. This figure illustrates that the dynamic compliance has decreased by 25.22%, from $f = 24.90\,\mathrm{N.m}$ for the initial distribution to $f = 18.62\,\mathrm{N.m}$ for the optimum topology configuration. In this example, maximum volume fraction of the MRE is set at V_0=50% with the initial values of the design variables set to ($x_i = 0.5$).

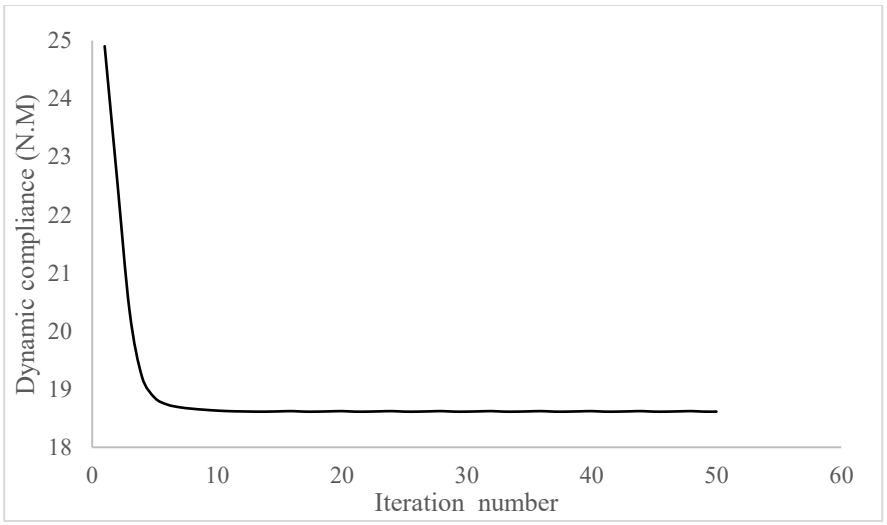

(a)

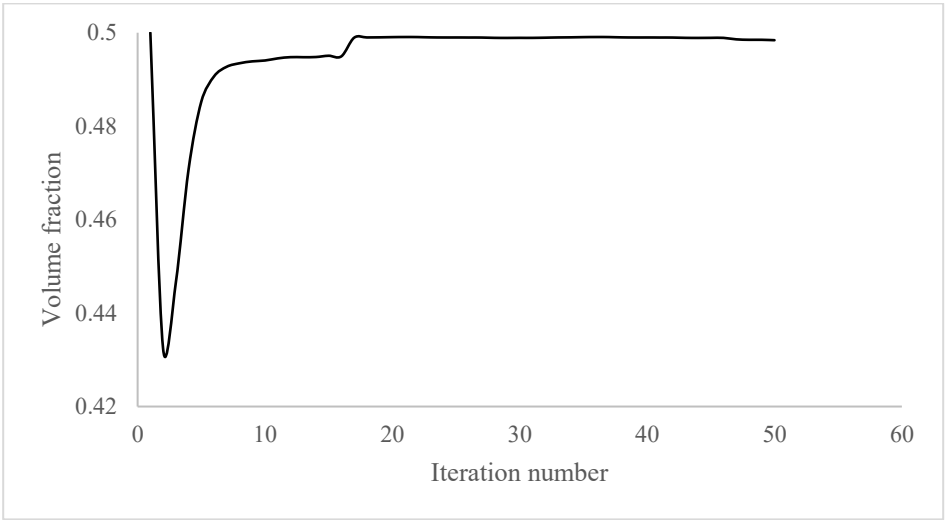

(b)

Figure 4-10: Optimization process history of MRE sandwich plate (CFCF): a) Convergence history of the dynamic compliance, b) Convergence history of the volume fraction (Case II)

Additionally, the impact of the volume fraction constraint on the optimal MRE topology has been explored, and the results for volume fractions of 0.1, 0.3, 0.5, and 0.7 are presented in Figure 4-14.

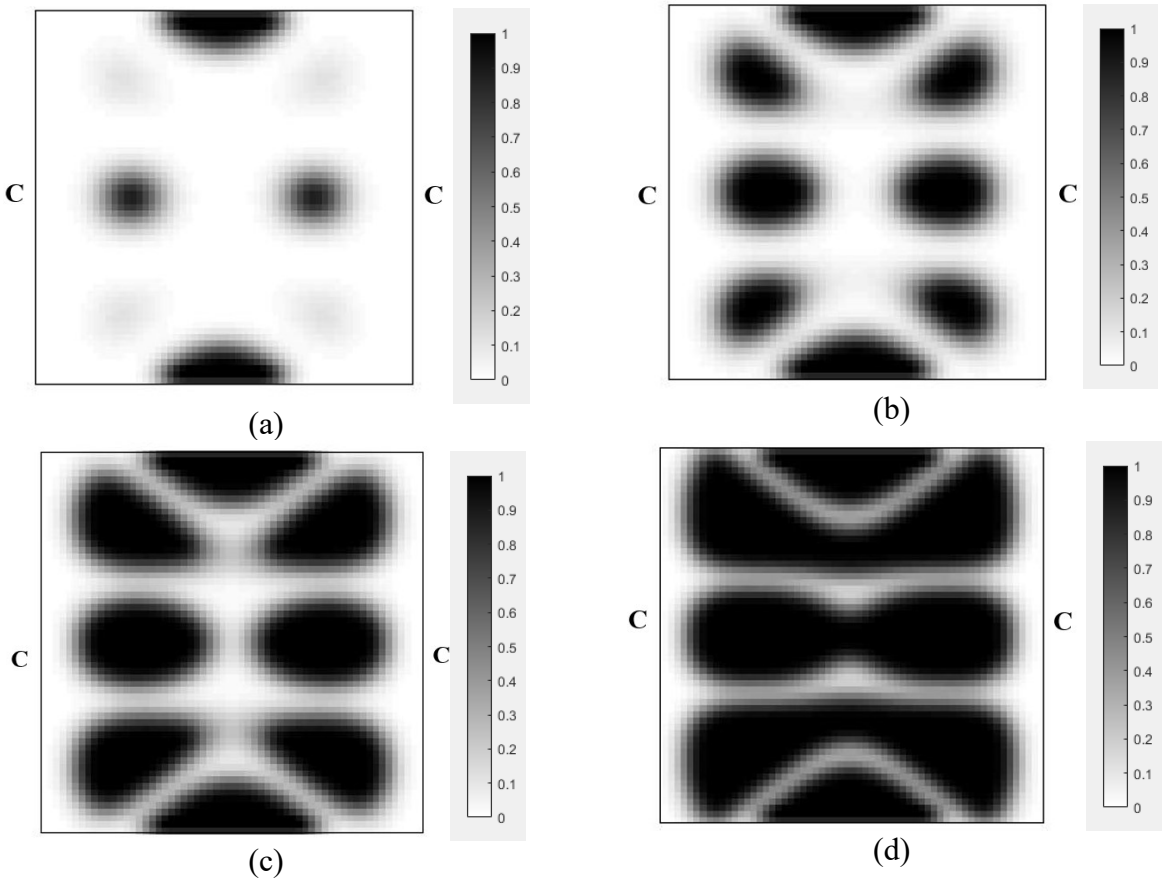

Figure 4-11: Optimal topology of the MRE layer for MRE sandwich plate (CFCF) under different volume constraints: a) 0.1; b) 0.3 c) 0.5 d) 0.7 (Case II).

The optimum objective functions for the aforementioned particular volume fractions are outlined in Table 4-5. Results show that despite a substantial increase in the volume fraction (from 0.1 to 0.7), there is only a 34.42% decrease in optimal dynamic compliance.

Table 4-5: The effect of volume fraction constraints on optimum dynamic compliance for MRE sandwich plate (CFCF) for Case II

Volume fraction	Optimum dynamic compliance (N.m)
0.1	27.31
0.3	21.16
0.5	18.78
0.7	17.91

Results for optimum topology of the MRE layer for Case II under different frequencies are also shown in Figure 4-15.

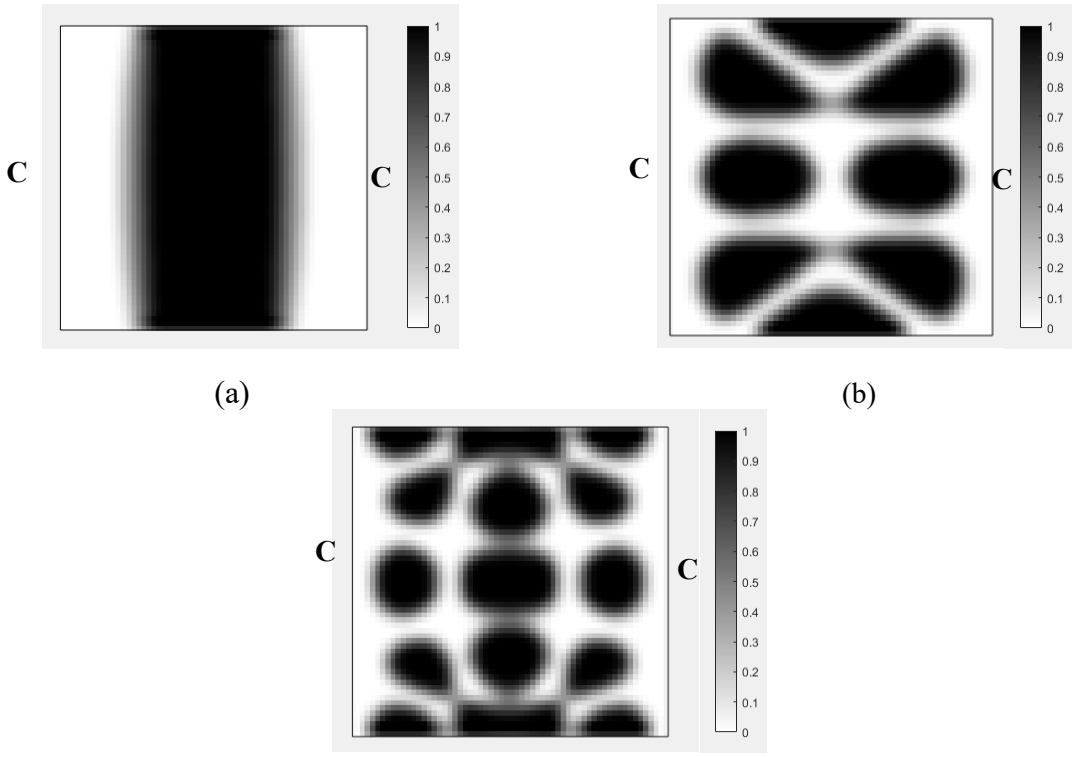

Figure 4-12: Optimal topology of the MRE layer MRE sandwich plate (CFCF) under different loading frequency: a) 45 Hz; b) 280 Hz; c) 440 Hz (Case II)

Case III: In this case, the MRE sandwich plate (CFCF) is under single concentrated harmonic loading at middle point B as shown in Figure 4-16 with similar magnitude of 1000 N as previous cases.

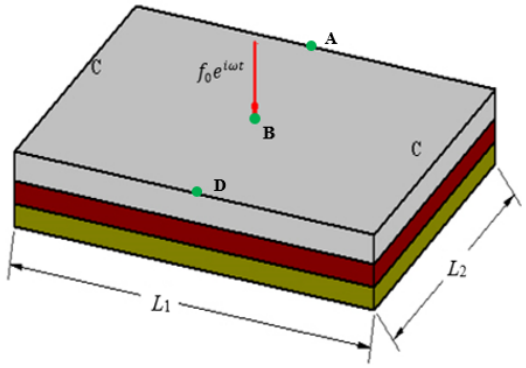

Figure 4-13: MRE sandwich plate (CFCF) with single loading position at B (Case III)

In this case, a similar examination was conducted, and the proposed topology optimization algorithm rapidly converged to the optimum solution, as shown in Figure 4-17. Examination of

results reveal a significant 26.78% decrease in dynamic compliance, from an initial value of f= 3.51 N·m to an optimal configuration of f= 2.57 N·m. Here, the maximum MRE volume fraction is set at V_0=50% with the initial values of the design variables set to ($x_i = 0.5$).

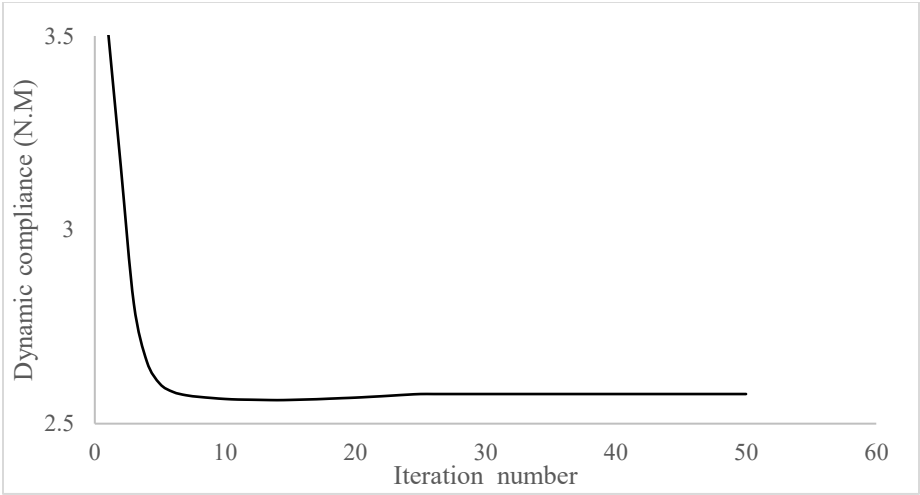

(a)

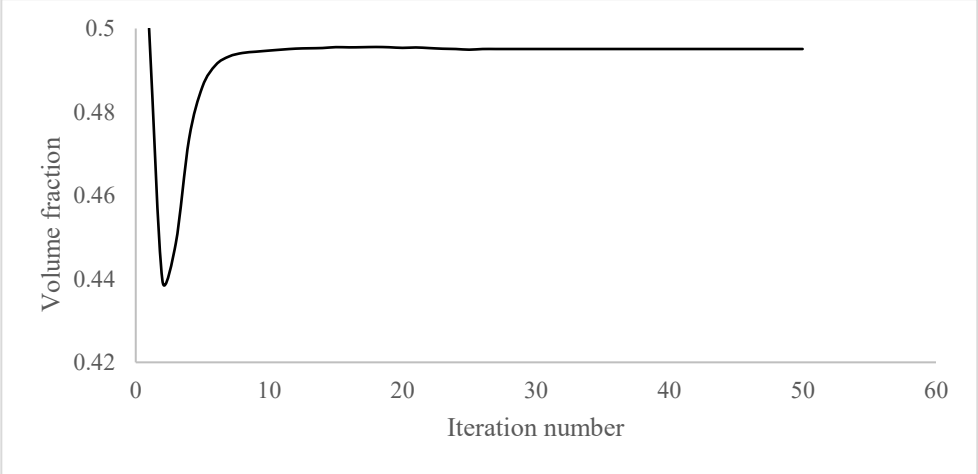

(b)

Figure 4-14: Optimization process history of MRE sandwich plate (CFCF): a) Convergence history of the dynamic compliance, b) Convergence history of the volume fraction (Case III)

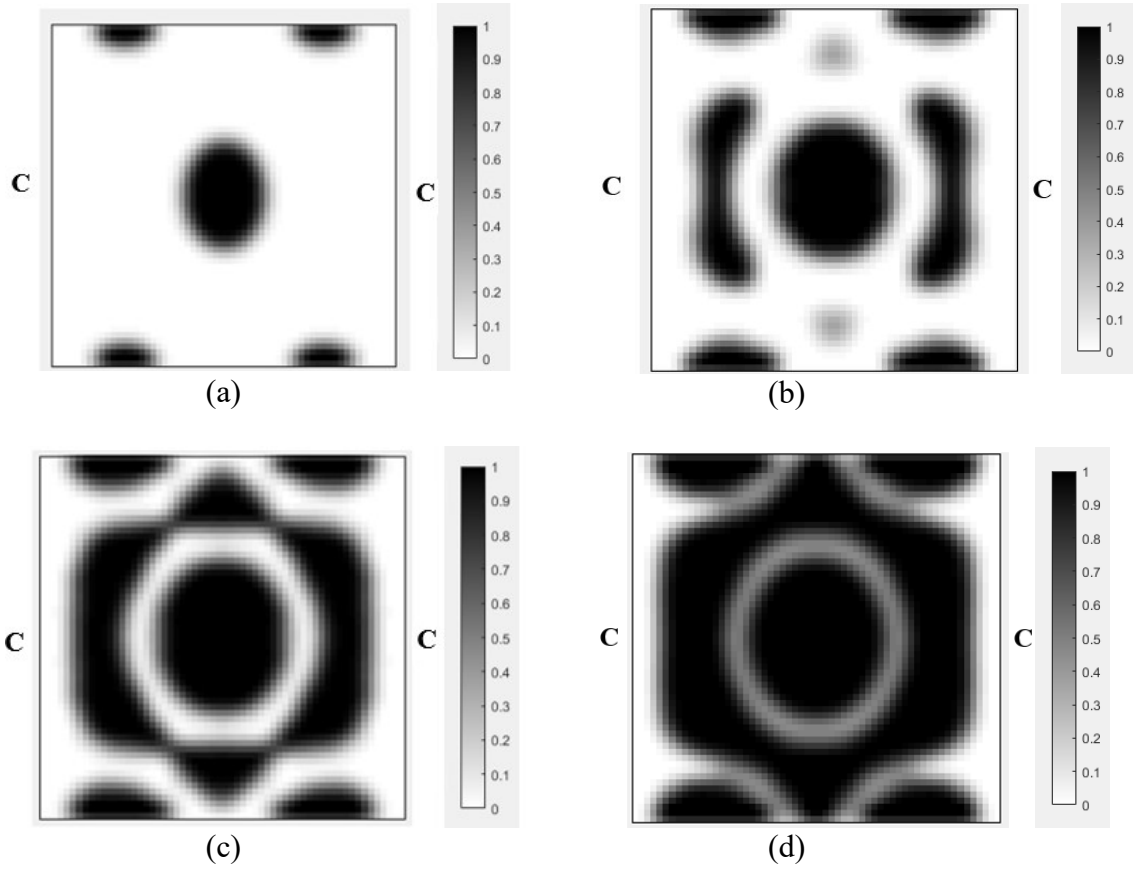

Figure 4-15: Optimal topology of the MRE layer for MRE sandwich plate (CFCF) under different volume constraints: a) 0.1; b) 0.3 c) 0.5 d) 0.7 (Case III).

The effect of the volume fraction constraint on the optimum topology of the MRE has also been investigated and results for the volume fractions of 0.1, 0.3, 0.5, 0.7 are shown in Figure 4-18. The optimum objective functions at the aforementioned volume fractions are given in Table 4-6.

Table 4-6: The effect of volume fraction constraints on optimum dynamic compliance for MRE sandwich plate (CFCF) for Case III

Volume fraction	Optimum dynamic compliance (N.m)
0.1	3.83
0.3	2.89
0.5	2.56
0.7	2.23

Results for optimum topology of the MRE layer for Case III under different frequencies are also shown in Figure 4-19.

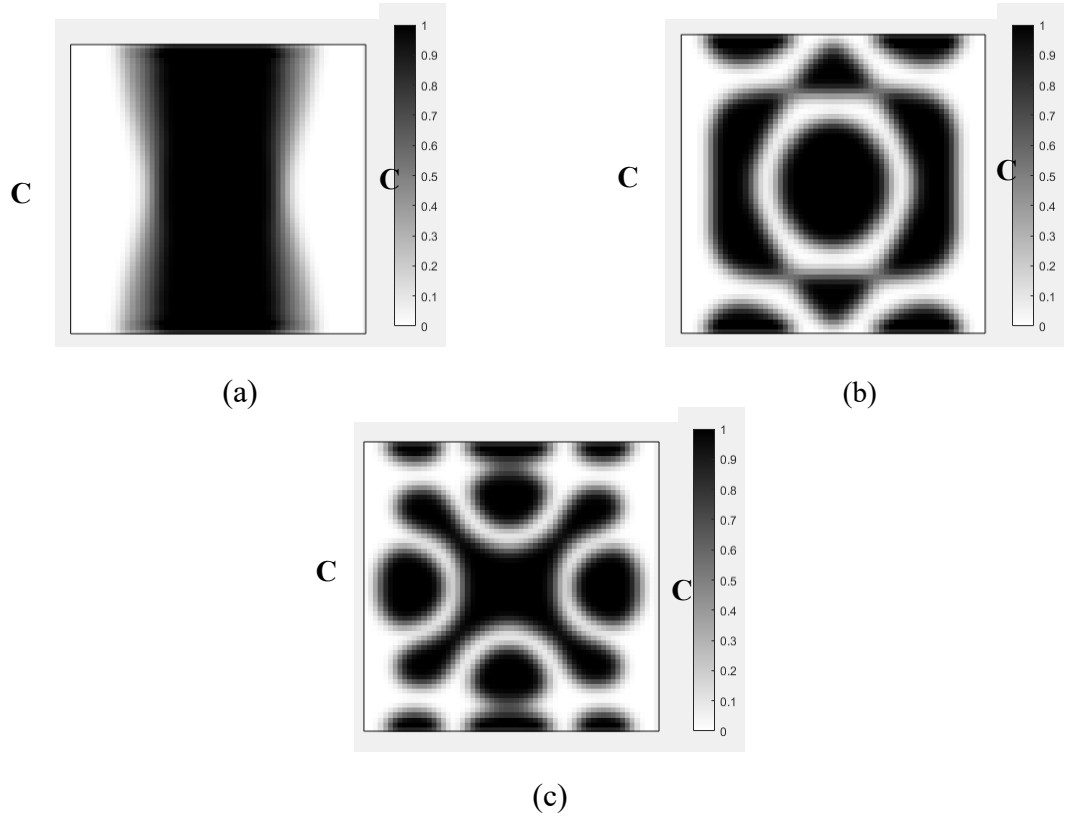

Figure 4-16: Optimal topology of the MRE layer MRE sandwich plate (CFCF) under different loading frequency: a) 45 Hz; b) 280 Hz; c) 440 Hz (Case III)

Case IV : Finally, the optimum topology of the MRE core layer in the MRE sandwich plate (CFCF) under single concentrated harmonic loading at edge point A as shown in Figure 4-20 is evaluated. The magnitude of the harmonic load is again kept at 1000 N.

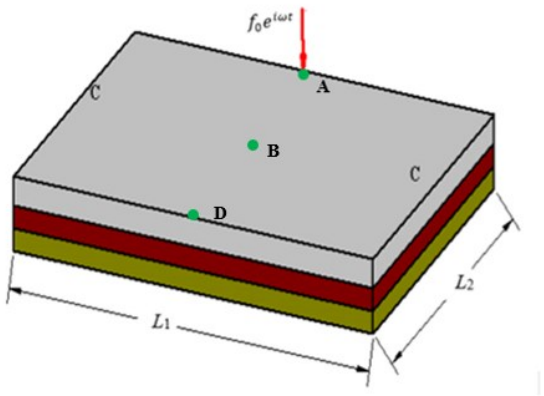

Figure 4-17: MRE sandwich plate (CFCF) with single loading position at A (Case IV)

Depicted in Figure 4-21, the developed topology optimization algorithm rapidly converged to the optimum solution. In this example, maximum volume fraction of the MRE is set at V_0=50% with the initial values of the design variables set to ($x_i = 0.5$). The figure highlights a substantial 50.49% reduction in dynamic compliance, transitioning from an initial value of f=5.07 N·m to an optimal configuration of f=2.51 N·m.

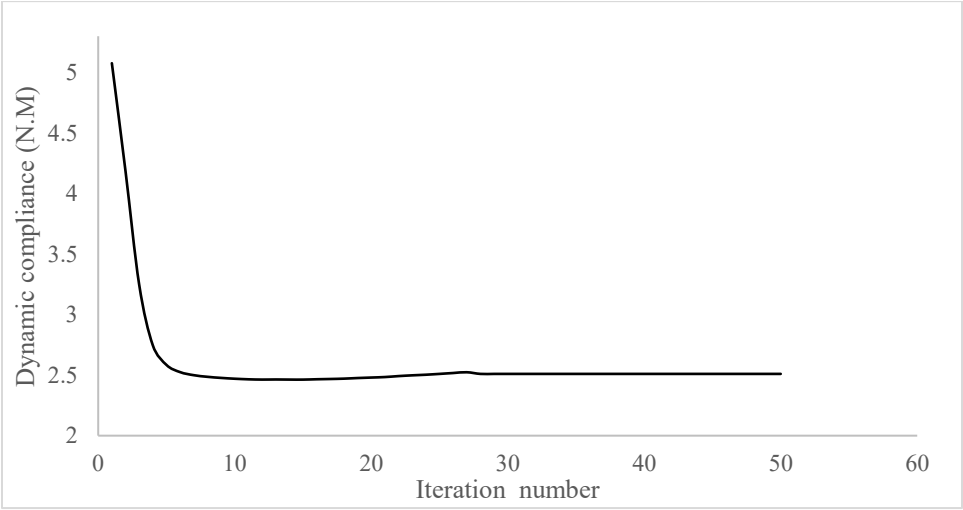

a

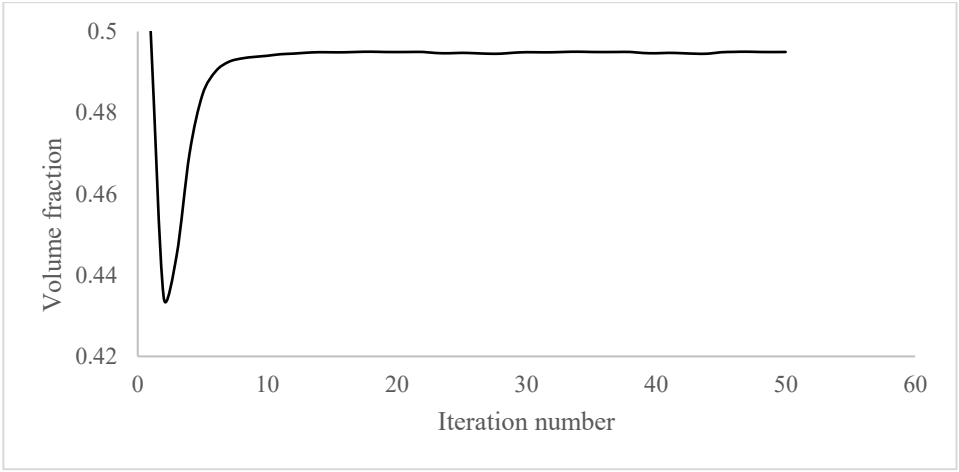

b

Figure 4-18: Optimization process history of MRE sandwich plate (CFCF): a) Convergence history of the dynamic compliance, b) Convergence history of the volume fraction (Case IV)

For this case, the optimum topologies for the volume fractions of 0.1, 0.3, 0.5, and 0.7 are shown in Figure 4-22, with the corresponding optimal objective functions provided in Table 4-7.

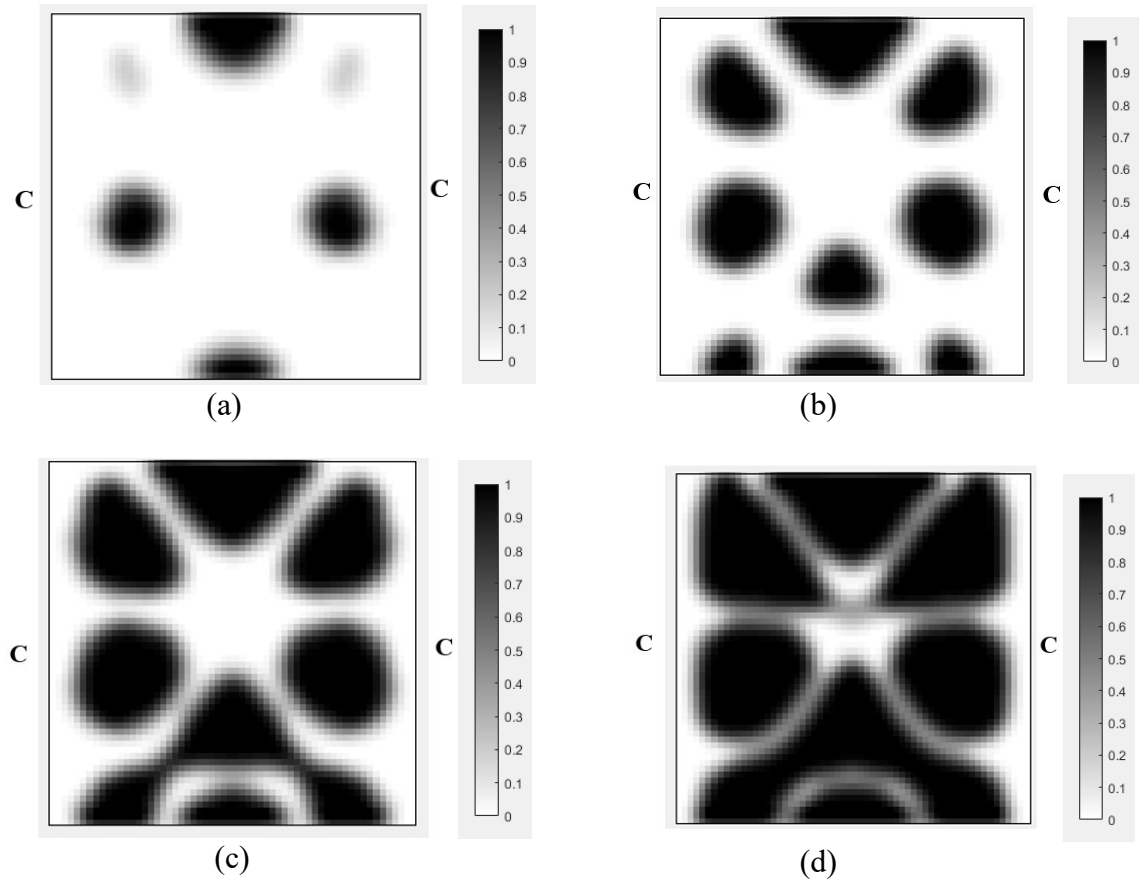

Figure 4-19: Optimal topology of the MRE layer for MRE sandwich plate (CFCF) under different volume constraints: a) 0.1; b) 0.3 c) 0.5 d) 0.7 (Case IV).

Table 4-7: The effect of volume fraction constraints on optimum dynamic compliance for MRE sandwich plate (CFCF) for Case IV

Volume fraction	Optimum dynamic compliance (N.m)
0.1	6.04
0.3	3.38
0.5	2.46
0.7	2.11

Results for optimum topology of the MRE layer for Case III under different frequencies are shown in Figure 4-23.

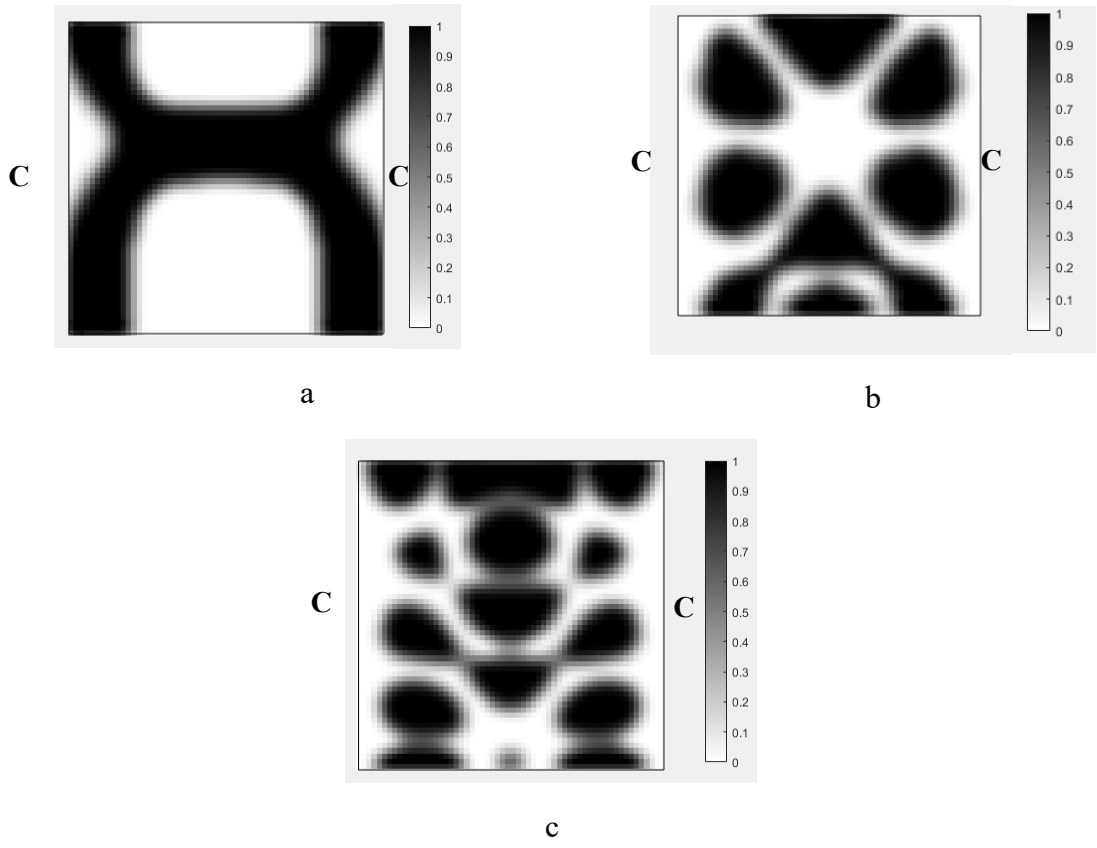

Figure 4-20: Optimal topology of the MRE layer MRE sandwich plate (CFCF) under different loading frequency: a) 45 Hz; b) 280 Hz; c) 440 Hz (Case IV)

Optimum topology results in Figures 4-11, 4-15, 4-19 and 4-23 illustrate the significant variations in optimal layouts of the MRE layer. These changes occur because different orders of eigenmodes are excited at different frequencies, resulting in different patterns for reducing the compliance. Furthermore, examination of results in Figures 4-10, 4-14, 4-18 and 4-22 shows that the optimum topology evolves and some isolated regions become connected as the volume fraction constraint on MRE increases. The optimum objective functions corresponding to different volume fractions, outlined in Table 4-4 to Table 4-7, represent that, as expected, a better control effectiveness can be achieved as more MR elastomer is used. However, it's important to note that using more MR elastomer also add excessive mass and increase the control effort.

4.4.3 Clamped-Free plate (CFFF)

In this example, a narrow MRE-sandwich plate clamped at one end and free at other sides (CFFF) subjected to harmonic loading at one free end as shown in Figure 4-24 is considered.

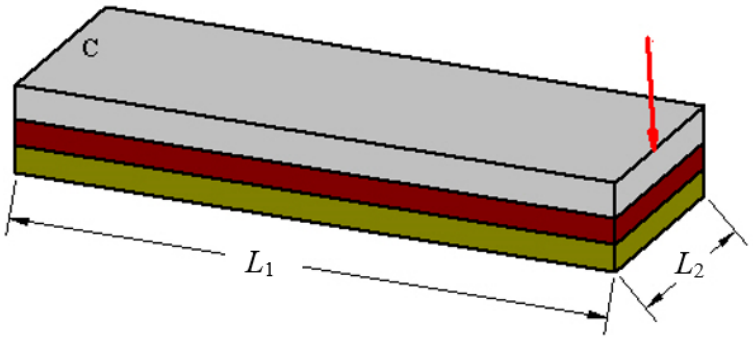

Figure 4-21: Cantilever MRE sandwich beam with loading exerted at the free end

Different layers of the MRE sandwich plate have the same properties as those in previous examples and provided in Table 4-3. The plate dimensions are $L_1 = 0.8$ m and $L_2 = 0.2$ m. The design domain is discretized using (80×22) elements. The applied harmonic load has a magnitude of 200 N. The optimum topology of the MRE layer for a volume fraction constraint of 0.5 is obtained for excitation frequencies of 80 and 380 Hz, as shown in Figure 4-25. Figure 4-26 represents the iteration history of the optimization problem for the case with the loading frequency of 80 Hz. The optimization process begins with the initial values of the design variables set to ($x_i = 0.5$). Examination of results reveal that there is a significant reduction in dynamic compliance, decreasing from 35.44 N·m for the initial design to 6.25 N·m for the optimized topology (82%).

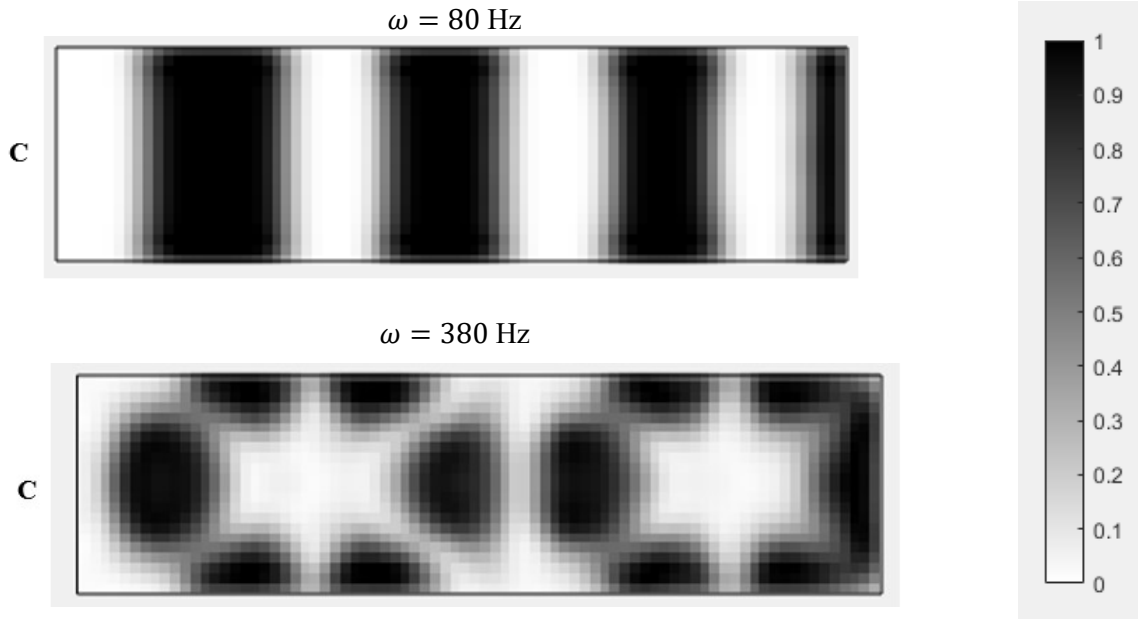

Figure 4-225: Optimal distribution of MRE layer for the clamped plate (CFFFF) under different frequency excitations

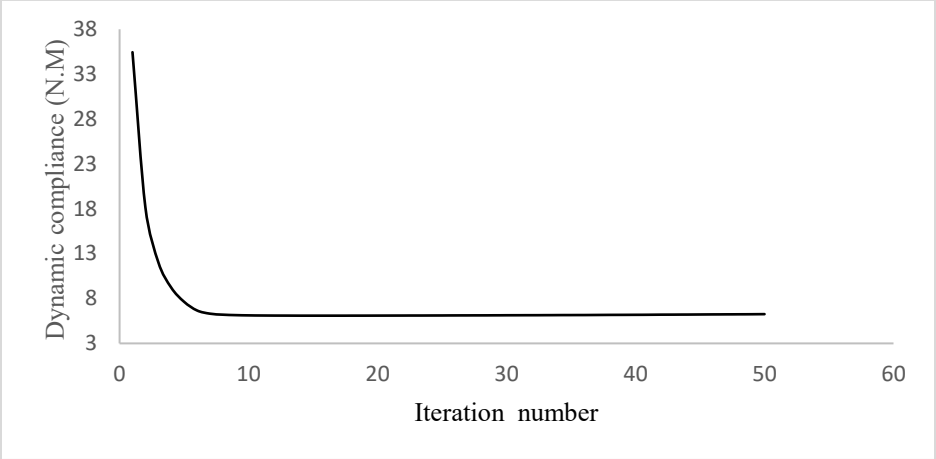

(a)

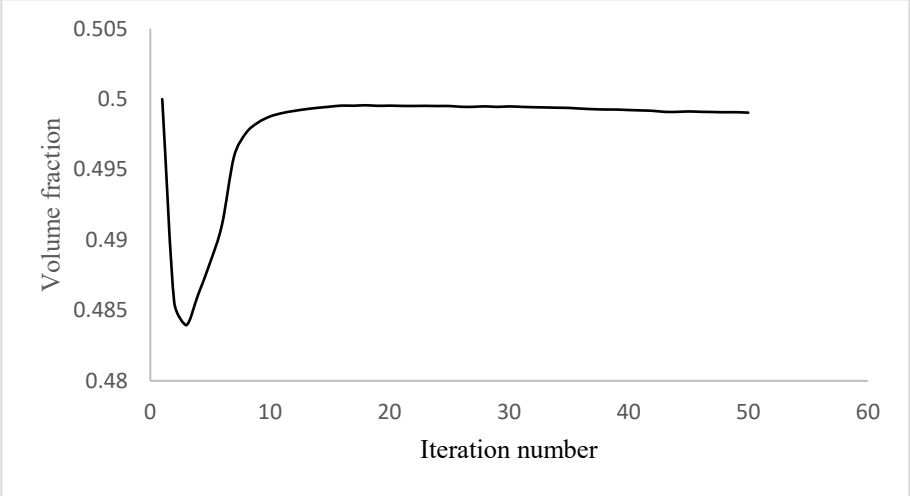

(b)

Figure 4-26: Optimization process history of clamped plate (CFFF): a) Convergence history of the dynamic compliance, b) Convergence history of the volume fraction

4.5 **Summary and Conclusion**

In this chapter, the accuracy of the proposed design optimization methodology to obtain the optimum topology of MRE layer in MRE-based sandwich structures to reach the maximum vibration suppression has been verified using benchmark test problems. The dynamic response of the structure is determined using the developed finite element model executed in MATLAB

environment. The accuracy of the FE model is confirmed by comparing the first four natural frequencies of the MRE-based sandwich plate using developed FE model and those reported in the literature with a maximum percentage error of 2.32%. Furthermore, the accuracy of the developed topology optimization algorithm is also investigated by comparing the optimized MR fluid layer distribution in a sandwich plate using the current proposed approach with those available in the literature

The developed finite element model and topology optimization technique have then been effectively used to evaluate topology distribution of MRE layer in MRE-sandwich plate under different harmonic loading and boundary conditions including SSSS, CCFF and CFFF. When applying the proposed optimization method to the MRE-based sandwich plate (SSSS) under harmonic loading with a magnitude of 1000 N and a frequency of 150 Hz, the dynamic compliance is reduced by 36.29% for the optimum topology with a volume fraction of 0.5.

Additionally, for the CCFF sandwich plate, it is observed that the dynamic compliance is reduced by 34% when subjected to harmonic loadings at the center of the plate and the middle of one of the free edges. The change in the location of the applied forces at different excitation frequencies results in a significant variation in the optimal layouts. This is mainly because different order of eigenmodes will be excited under different frequencies, leading to distinct patterns for suppressing the vibration level of the structure.

Lastly, optimum topology of the MRE layer for a clamped MRE sandwich plate (CFFF), under concentrated harmonic loading with magnitude of 200 N at the free end and two different excitation frequencies, has been evaluated. In this case, for 80 Hz excitation frequency, a 82% decrease in dynamic compliance is observed for the optimal topology with a volume fraction of 0.5. These results highlight the success of the proposed method in achieving the optimum distribution of the MRE layer for minimizing dynamic compliance and subsequently reducing structural vibrations.

Chapter 5: Contributions, Conclusions and Future Remarks

5.1 Major Contributions

The present research dissertation provides a comprehensive investigation of the vibration characteristics of MRE-based sandwich plates and the achievement of the optimal configuration of the MRE layer for vibration reduction of the structure. The major contributions of the dissertation research are summarized below:

- A numerical model based on the FE method is developed to analyze dynamic and vibration characteristics of MRE-based sandwich plates under varying magnetic fields. To validate the accuracy of the numerical model, the obtained dynamic characteristics of the plate in terms of the natural frequencies are compared with those reported in existing literature.
- A density-based topology optimization approach for obtaining the optimum topology of MRE layer in MRE-based sandwich plates for the maximum vibration suppression of the structure is proposed. In this approach, MMA is applied as the design updating algorithm. Furthermore, to interpolate the behavior of the MRE material, the MREP method which is an extension of the SIMP method is proposed. This approach allows for effective material interpolation in the optimization process. By applying the proposed optimization method, the optimum topologies of the MRE layer in the sandwich plate under different loading conditions, as well as various boundary conditions are obtained.

5.2 Major Conclusions

The following are the major conclusions drawn from the findings of this research dissertation:

- Fully MRE-covered sandwich structures generally provide better vibration control performance compared to partially-covered ones. However, optimal MRE treatment can achieve significant damping with relatively lower mass, indicating the potential for efficient design.
- The MREP model, proposed for material interpolation, is an effective model in the optimization process. It aids in achieving desired material properties in the design of MRE-treated structures.

- In the case of harmonic loading, the excitation frequency plays a crucial role in determining the optimal arrangement of the MRE layer. The frequency affects the performance and effectiveness of the MRE treatment.
- Modifying the volume fraction of the MRE layer in the optimization process results in similar optimal topologies, except for certain isolated parts that become connected as the volume fraction increases.
- MMA is a fast convergence method commonly used in topology optimization problems. It facilitates efficient optimization and convergence towards optimal solutions.
- The combination of the finite element method and the MMA can be effectively used for topology optimization, regardless of the boundary conditions, loading conditions, and the type of structure.
- The application of MREs in sandwich structures subjected to a magnetic field can significantly alter the stiffness and damping properties of the structures. The field-dependent viscoelastic properties of MREs l can be exploited to enhance the performance and functionality of sandwich structures in various applications.

5.3 Future Remarks

In this dissertation, topology optimization of MRE layer in sandwich structures as well as their dynamic characteristics are investigated. The developed topology optimization methodology can be effectively used to identify the optimum layout of MRE layer in sandwich plates with different boundary conditions and varying excitation frequencies. The method, however, needs to be further refined so as to extend to general structures and loading conditions. Some of the recommended studies are suggested below:

- Examination of MMA and GMAA combination: The combination of MMA and GMAA should be further investigated to cover a wider range of frequency loading conditions and accelerate the optimization process. This can enhance the effectiveness and efficiency of the optimization problem.
- Addition of more variables: The optimization problem can be expanded by including more variables such as temperature, magnetic field density, and excitation frequency. This will

enable obtaining the optimum topology for a range of variables, enhancing the adaptability of the optimized structure.

- MRE-based sandwich plates as adaptive tunable vibration absorbers: The application of MRE sandwich plates as adaptive tunable vibration absorbers should be explored. Investigating their effectiveness in reducing vibrations and their adaptability to varying conditions can provide valuable insights for practical applications.
- Experimental verification of optimum topologies: The obtained optimum topologies from the optimization process can be experimentally verified to assess their impact on vibration reduction compared to the initial layout. This experimental validation helps to further validate the effectiveness of the optimization approach.
- Dynamic characterization at various conditions: The dynamic characteristics of MRE sandwich plates under various temperatures and magnetic fields should be investigated. This analysis helps understand how different conditions affect the performance and behavior of the structure.

References

[1] O. El-Khoury and H. Adeli, "Recent Advances on Vibration Control of Structures Under Dynamic Loading," *Archives of Computational Methods in Engineering*, vol. 20, no. 4, pp. 353–360, Oct. 2013.

[2] K. Wang and Y. Kim, "Semi-active vibration control of structures via variable damping elements," *Mechanical Systems and Signal Processing*, Sep. 1991.

[3] A. Preumont, *Vibration Control of Active Structures: An Introduction*. 2014. [Online]. Available: http://cds.cern.ch/record/2013290.

[4] J. Qiu, H. Ji, and K. Zhu, "Semi-active vibration control using piezoelectric actuators in smart structures," *Frontiers of Mechanical Engineering in China*, May 2009.

[5] J.-H. Kim, "Multifunctional Smart Biopolymer Composites as Actuators," in *Elsevier eBooks*, 2017, pp. 311–331.

[6] Surbhi and Sukesha, "Response of piezoelectric materials to the external temperature, electric field and humidity," *Materials Today: Proceedings*, Jan. 2020.

[7]A. Bahmani, G. Li, T.L. Willett, J. Montesano, "Generating realistic representative microstructure of biomimetic composite materials for computational assessment of mechanical properties". *Mater. Today Proc.*, vol 7, pp. 373–381, Jan. 2019.

[8] G. Carotenuto, G. La Peruta, and L. Nicolais, "Thermo-chromic materials based on polymer-embedded silver clusters," *Sensors and Actuators B-chemical*, vol. 114, no. 2, pp. 1092–1095, Apr. 2006.

[9] X. Yuan et al., "A stable high-performance isotropic electrorheological elastomer towards controllable and reversible circular motion," *Composites Part B-engineering*, vol. 193, p. 107988, Jul. 2020.

[10] M. Usman, I. Y. Kim, and H.-J. Jung, "Improving thermoelectric energy harvesting efficiency by using graphene," *AIP Advances*, vol. 6, no. 5, p. 055027, May 2016.

[11] S. Jiang, J. Ichihashi, H. Monobe, M. Fujihira, and M. Ohtsu, "Highly localized photochemical processes in LB films of photo chromic material by using a photon scanning tunneling microscope," *Optics Communications*, vol. 106, no. 4–6, pp. 173–177, Mar. 1994.

[12] B. Wang and L. Kari, "A visco-elastic-plastic constitutive model of isotropic magneto-sensitive rubber with amplitude, frequency and magnetic dependency," *International Journal of Plasticity*, vol. 132, p. 102756, Sep. 2020

[13] M. V. Vaganov, D. Borin, S. Odenbach, and Yu. L. Raikher, "Training effect in magnetoactive elastomers due to undermagnetization of magnetically hard filler," *Physica B-condensed Matter*, vol. 578, p. 411866, Feb. 2020.

[14] C. Velmurugan, V. Senthilkumar, J. Kesavan, and K. Ramya, "Effects of sintering temperature on grain growth of NiTiCu shape memory alloy," *Materials Today: Proceedings*, vol. 39, pp. 1570–1574, Jan. 2021.

[15] S. K. Kang, K. Choi, J.-D. Nam, and H. J. Choi, "Magnetorheological Elastomers: Fabrication, Characteristics, and Applications," *Materials*, vol. 13, no. 20, p. 4597, Oct. 2020.
[16] A. G. Olabi and A. Grunwald, "Design and application of magneto-rheological fluid," *Mater. Des*, vol. 28, no. 10, pp. 2658–2664, Jan. 2007.
[17] J. D. Carlson and M. Jolly, "MR fluid, foam and elastomer devices," *Mechatronics*, vol. 10, no. 4–5, pp. 555–569, Jun. 2000.
[18] M. K. Thakur and C. Sarkar, "Influence of Graphite Flakes on the Strength of Magnetorheological Fluids at High Temperature and its Rheology," *IEEE Transactions on Magnetics*, vol. 56, no. 5, pp. 1–10, May 2020.
[19] M. Cho, S. S. Lim, I.-K. Jang, H. H. F. Choi, and M. S. Jhon, "Encapsulation of Spherical Iron-Particle With PMMA and Its Magnetorheological Particles," *IEEE Transactions on Magnetics*, vol. 40, no. 4, pp. 3036–3038, Jul. 2004.
[20] W. H. Chuah, W. Zhang, H. J. Choi, and Y. Seo, "Magnetorheology of Core–Shell Structured Carbonyl Iron/Polystyrene Foam Microparticles Suspension with Enhanced Stability," *Macromolecules*, vol. 48, no. 19, pp. 7311–7319, Sep. 2015.
[21] T. Liu and Y. Xu, "Magnetorheological Elastomers: Materials and Applications," *in IntechOpen eBooks*, 2019.
[22] J. E. Japka, "Microstructure and Properties of Carbonyl Iron Powder," *JOM*, vol. 40, no. 8, pp. 18–21, Aug. 1988.
[23] L. X. Chen, X. Gong, W. Jiang, J. Yao, H. Deng, and W. Li, "Investigation on magnetorheological elastomers based on natural rubber," *Journal of Materials Science*, vol. 42, no. 14, pp. 5483–5489, Apr. 2007.
[24] H. Böse, "Viscoelastic Properties of Silicone-Based Magnetorheological Elastomer," *International Journal of Modern Physics B*, vol. 21, no. 28n29, pp. 4790–4797, Nov. 2007.
[25] T. Tian, X. Zhang, W. Li, G. Alici, and J. L. Ding, "Study of PDMS based magnetorheological elastomers," *Journal of Physics: Conference Series*, vol. 412, p. 012038, Feb. 2013.
[26] X. Gong, X. Y. Zhang, and P. Zhang, "Fabrication and characterization of isotropic magnetorheological elastomers," Polymer Testing, vol. 24, no. 5, pp. 669–676, Aug. 2005.
[27] Zhu H. Fabrication of practical magnetorheological fluids and their properties [thesis]. Hefei: University of Science and Technology of China; 2010.
[28] B. Nayak, R. Das, and S. S. Gautam, "Vibration performances of MRE embedded sandwich beam: experimental study," *Vibroengineering Procedia*, vol. 21, pp. 20–25, Dec. 2018.
[29] V. R. Babu and R. Vasudevan, "Dynamic analysis of tapered laminated composite magnetorheological elastomer (MRE) sandwich plates," *Smart Materials and Structures*, vol. 25, no. 3, p. 035006, Feb. 2016.
[30] W.J. Choi, Y.P. Xiong, R.A. Shenoi, "Vibration characteristics of smart sandwich beams embedded with magnetorheological elastomer cores," *Advancements in Marine Structures: Proceedings of the 1st MARSTRUCT International Conference,* pp. 421-428, May 2007.
[31] Z. Ying and Y. Ni, "Micro-vibration response of a stochastically excited sandwich beam with a magnetorheological elastomer core and mass," *Smart Materials and Structures*, vol. 18, no. 9, p. 095005, Jul. 2009.
[32] H. Li, W. Wang, Q. Wang, "Static and dynamic performances of sandwich plates with magnetorheological elastomer core: Theoretical and experimental studies," *Journal of Sandwich Structures and Materials*, vol. 24, no. 3, pp. 1556–1579, Jan. 2022.

[33] R. B. Vemuluri, V. Rajamohan, and P. E. Sudhagar, “Structural optimization of tapered composite sandwich plates partially treated with magnetorheological elastomers,” *Composite Structures*, vol. 200, pp. 258–276, Sep. 2018.
[34] J. Snamina, “Optimal location of an active segment of magnetorheological fluid layer in a sandwich plate,” *12th International Carpathian Control Conference (ICCC)*, pp. 362-365, 2011.
[35] O. Sigmund and K. Maute, “Topology optimization approaches,” *Structural and Multidisciplinary Optimization*, vol. 48, no. 6, pp. 1031–1055, Aug. 2013.
[36] A. Homayouni-Amlashi, T. Schlinquer, A. Mohand-Ousaid, and M. Rakotondrabe, “2D topology optimization MATLAB codes for piezoelectric actuators and energy harvesters,” Structural and Multidisciplinary Optimization, vol. 63, no. 2, pp. 983–1014, Oct. 2020.
[37] R. Ahmad and H. K. Voruganti, “Structural Topology Optimization: Methods and Applications,” *in Lecture notes in mechanical engineering*, Springer Nature, 2020.
[38] M. P. Bendsøe, “Optimal shape design as a material distribution problem,” Structural Optimization, vol. 1, no. 4, pp. 193–202, Dec. 1989.
[39] M. P. Bendsøe and O. Sigmund, *Topology Optimization: Theory, Methods, and Applications*. 2011. [Online]. Available: http://ci.nii.ac.jp/ncid/BA59288628.
[40] B. Bourdin, “Filters in topology optimization,” *International Journal for Numerical Methods in Engineering*, vol. 50, no. 9, pp. 2143–2158, Jan. 2001.
[41] Z. Kang, X. Zhang, S.-G. Jiang, and G. Cheng, “On topology optimization of damping layer in shell structures under harmonic excitations,” *Structural and Multidisciplinary Optimization*, vol. 46, no. 1, pp. 51–67, Dec. 2011.
[42] S. Y. Kim, C. K. Mechefske, and I. Kim, “Optimal damping layout in a shell structure using topology optimization,” *Journal of Sound and Vibration*, vol. 332, no. 12, pp. 2873–2883, Jun. 2013.
[43] D. Guzmán, E. C. N. Silva, and W. M. Rubio, “Topology optimization of piezoelectric sensor and actuator layers for active vibration control,” *Smart Materials and Structures*, vol. 29, no. 8, p. 085009, Jun. 2020.
[44] A. Homayouni-Amlashi, T. Schlinquer, A. Mohand-Ousaid, and M. Rakotondrabe, “2D topology optimization MATLAB codes for piezoelectric actuators and energy harvesters,” *Structural and Multidisciplinary Optimization*, vol. 63, no. 2, pp. 983–1014, Oct. 2020.
[45] J.-W. Noh and G. H. Yoon, “Topology optimization of piezoelectric energy harvesting devices considering static and harmonic dynamic loads,” *Advances in Engineering Software*, vol. 53, pp. 45–60, Nov. 2012.
[46] K. Svanberg, “The method of moving asymptotes—a new method for structural optimization,” *International Journal for Numerical Methods in Engineering*, vol. 24, no. 2, pp. 359–373, Feb. 1987.
[47] J.-Y. Yeh and L. Chen, “Finite element dynamic analysis of orthotropic sandwich plates with an electrorheological fluid core layer,” *Composite Structures*, vol. 78, no. 3, pp. 368–376, May 2007.
[48] Z. Huang, Z. Qin, and F. Chu, “Vibration and damping characteristics of sandwich plates with viscoelastic core,” *Journal of Vibration and Control*, vol. 22, no. 7, pp. 1876–1888, Aug. 2014
[49] E. Reissner, “The Effect of Transverse Shear Deformation on the Bending of Elastic Plates,” *Journal of Applied Mechanics*, vol. 12, no. 2, pp. A69–A77, Jun. 1945.

[50] R. D. Mindlin, “Influence of Rotatory Inertia and Shear on Flexural Motions of Isotropic, Elastic Plates,” Journal of Applied Mechanics, vol. 18, no. 1, pp. 31–38, Mar. 1951.
[51] P. K. Srivastava, S. Shukla “Structural Optimization Methods: A General Review” *IJIRSET*, vol. 6, no. 9, pp. 88–92, May 2017.
[52] M. P. Bendsoe and O. Sigmund, Topology Optimization: Theory, Methods, and Applications. Springer Science & Business Media, 2013.
[53] T. Zhan, “Progress on different topology optimization approaches and optimization for additive manufacturing: a review,” *Journal of Physics*, vol. 1939, no. 1, p. 012101, May 2021.
[54] H. A. Eschenauer, V. Kobelev, and A. Schumacher, “Bubble method for topology and shape optimization of structures,” *Structural Optimization*, vol. 8, no. 1, pp. 42–51, Aug. 1994.
[55] T. Yamada, K. Izui, S. Nishiwaki, and A. Takezawa, “A topology optimization method based on the level set method incorporating a fictitious interface energy,” *Computer Methods in Applied Mechanics and Engineering*, vol. 199, no. 45–48, pp. 2876–2891, Nov. 2010.
[56] S. Osher and J. A. Sethian, “Fronts propagating with curvature-dependent speed: Algorithms based on Hamilton-Jacobi formulations,” *Journal of Computational Physics*, vol. 79, no. 1, pp. 12–49, Nov. 1988.
[57] M. P. Bendsøe, “Optimal shape design as a material distribution problem,” *Structural Optimization*, vol. 1, no. 4, pp. 193–202, Dec. 1989.
[58] J. Alexandersen, “A detailed introduction to density-based topology optimisation of fluid flow problems with implementation in MATLAB,” *Structural and Multidisciplinary Optimization*, vol. 66, no. 1, Dec. 2022.
[59] O. C. Zienkiewicz, R. J. K. Taylor, and J. Z. Zhu, *The Finite Element Method: its Basis and Fundamentals*. 2013.
[60] E. Reissner, “On the Theory of Bending of Elastic Plates,” *Journal of Mathematics and Physics*, vol. 23, no. 1–4, pp. 184–191, Apr. 1944.
[61] E. Holmberg, B. Torstenfelt, and A. Klarbring, “Stress constrained topology optimization,” *Structural and Multidisciplinary Optimization*, vol. 48, no. 1, pp. 33–47, Feb. 2013.
[62] M. P. Bendsøe and O. Sigmund, “Material interpolation schemes in topology optimization,” *Archive of Applied Mechanics*, vol. 69, no. 9–10, pp. 635–654, Nov. 1999.
[63] M. P. Bendsøe, “Optimal shape design as a material distribution problem,” *Structural Optimization*, vol. 1, no. 4, pp. 193–202, Dec. 1989.
[64] G. I. N. Rozvany, M. Zhou, and T. Birker, “Generalized shape optimization without homogenization,” *Structural Optimization*, vol. 4, no. 3–4, pp. 250–252, Sep. 1992.
[65] O. Sigmund, “On the Design of Compliant Mechanisms Using Topology Optimization,” *Mechanics of Structures and Machines*, vol. 25, no. 4, pp. 493–524, Jan. 1997.
[66] E. Andreassen, A. Clausen, M. Schevenels, B. S. Lazarov, and O. Sigmund, “Efficient topology optimization in MATLAB using 88 lines of code,” Structural and Multidisciplinary Optimization, vol. 43, no. 1, pp. 1–16, Nov. 2010.
[67] N. Wang and X. Y. Zhang, *A Solid Isotropic Material with Parallel Penalization method for structural topology optimization with multiple materials*. 2016.
[68] Z.-D. Ma, N. Kikuchi, and I. Hagiwara, “Structural topology and shape optimization for a frequency response problem,” *Computational Mechanics*, vol. 13, no. 3, pp. 157–174, Dec. 1993.
[69] M.P. Bendsøe, N. Kikuchi, “Generating optimal topologies in structural design using a homogenization method,” *Comput. Methods Appl. Mech. Eng.*, vol 71, no 2, pp. 197-224, Aug. 1988.

[70] A. Homayouni-Amlashi, T. Schlinquer, A. Mohand-Ousaid, “2D topology optimization MATLAB codes for piezoelectric actuators and energy harvesters,” *Struct Multidisc Optim*, vol 63, pp. 983–1014, 2021.
[71] K. Svanberg, “The method of moving asymptotes—a new method for structural optimization,” *International Journal for Numerical Methods in Engineering*, vol. 24, no. 2, pp. 359–373, Feb. 1987.
[72] N. Kim, T. Dong, D. Weinberg, and J. Dalidd, “Generalized Optimality Criteria Method for Topology Optimization,” Applied Sciences, vol. 11, no. 7, p. 3175, Apr. 2021.
[73] T. Jiang and P. Y. P. Ambros, “A First Order Method Of Moving Asymptotes For Structural Optimization,” *WIT Transactions on the Built Environment*, vol. 14, Jan. 1970.
[74] K. Svanberg, Mma and gcmma-two methods for nonlinear optimization, *Technical report, Optimization and Systems Theory 1*, Sep 2007.
[75] H. Zhang, X. Ding, W. Ni, Y. Chen, X. Zhang, H. Li, “Concurrent Topology Optimization of Composite Plates for Minimum Dynamic Compliance, ” *Materials*, vol 15, p. 538, 2022.
[76] J.-Y. Yeh, “Vibration analysis of sandwich rectangular plates with magnetorheological elastomer damping treatment,” *Smart Materials and Structures*, vol. 22, no. 3, p. 035010, Feb. 2013.
[77] X. Zhang and Z. Kang, “Topology optimization of magnetorheological fluid layers in sandwich plates for semi-active vibration control,” *Smart Materials and Structures*, vol. 24, no. 8, p. 085024, Jul. 2015.
[78] A. Rasooli, R. Sedaghati, and M. Hemmatian, “A novel magnetorheological elastomer-based adaptive tuned vibration absorber: design, analysis and experimental characterization,” *Smart Materials and Structures,* vol. 29, no. 11, p. 115042, Oct. 2020.

Appendix A

Referring to Eq. (2.29), the elemental stiffness matrix includes extensional and bending matrixes corresponding to each layer defined respectively as:

$$k_{Ti} = h_i \int_A {B_{Ti}}^T D_{Ti} B_{Ti} dA$$
$$k_{bi} = h_i \int_A {B_{bi}}^T D_{bi} B_{bi} dA \tag{A.1}$$

where,

$$B_{Tc} = \left[\frac{\partial N_1}{\partial x} \quad \frac{\partial N_2}{\partial y} \quad \frac{\partial N_1}{\partial y} + \frac{\partial N_2}{\partial x}\right]^T$$
$$B_{Tm} = \left[\frac{\partial N_8}{\partial x} \quad \frac{\partial N_9}{\partial y} \quad \frac{\partial N_8}{\partial y} + \frac{\partial N_9}{\partial x}\right]^T \tag{A.2}$$
$$B_{Tb} = \left[\frac{\partial N_3}{\partial x} \quad \frac{\partial N_4}{\partial y} \quad \frac{\partial N_3}{\partial y} + \frac{\partial N_4}{\partial x}\right]^T$$

It is noted that the indexes *c*, *m* and *b* are used to represent the constraining, MRE and the basic layers, respectively.

And for the bending term the associated matrix is yield as:

$$B_{bi} = \left[\frac{\partial^2 N_5}{\partial x^2} \quad \frac{\partial^2 N_5}{\partial y^2} \quad 2\frac{\partial^2 N_5}{\partial xy}\right]^T \tag{A.3}$$

Also, the shear stiffness matrix of the MRE layer is defined as:

$$k_{sm} = h_m \int_A {B_{sm}}^T G B_{sm} dA$$
$$B_{sm} = \begin{bmatrix} N_{10} \\ N_{11} \end{bmatrix} \tag{A.4}$$

Similarly, for the elemental mass matrix, the extension and bending stiffness terms are obtained as:

$$m_{bc} = \rho_c h_c \int_A ({N_1}^T N_1 + {N_2}^T N_2) dA$$
$$m_{bb} = \rho_b h_c \int_A ({N_3}^T N_3 + {N_4}^T N_4) dA$$
$$m_{bm} = \rho_m h_c \int_A ({N_8}^T N_8 + {N_9}^T N_9) dA \tag{A.5}$$
$$m_{bi} = \rho_i h_i \int_A {N_5}^T N_5 dA$$